CONFORMATIONS OF THE REPEAT PEPTIDES OF ELASTIN IN SOLUTION: AN APPLICATION OF PROTON AND CARBON-13 MAGNETIC RESONANCE TO THE DETERMINATION OF POLYPEPTIDE SECONDARY STRUCTURE

Authors: **D. W. Urry***
M. M. Long
Laboratory of Molecular Biophysics and the
Cardiovascular Research and Training Center
University of Alabama Medical Center
Birmingham, Alabama

Referee: Erhard Gross
Public Health Service
National Institutes of Health
Bethesda, Maryland

I. INTRODUCTION

The elastic fiber provides the resilience required of such tissues as ligaments, skin, lung, and blood vessel walls. In the ligamentum nuchae, fibrous elastin constitutes more than 70% of the total dry weight, and in the major elastic arteries, e.g., the descending thoracic aorta, there is twice as much elastin as collagen, the other major connective tissue protein. The elastic fiber of vascular wall takes on additional importance as it is a primary site for vascular pathology.[1-24] This is particularly significant since major cardiovascular diseases are the cause of more than 50% of all deaths in this country.

The elastic fiber is comprised of an insoluble core of about 6μ diameter[25] which is coated by microfibrillar glycoprotein.[26] The fibrous elastin of the core is formed from a single protein which becomes highly cross-linked by means of desmosine, isodesmosine, and lysinonorleucine residues derived from reactions of lysine side chains of the precursor protein.[27-30] Tropoelastin, the precursor protein, has been isolated[31, 32] and partially sequenced.[33,34] With the sequence determined for about one half of the approximately 70,000-dalton tropoelastin, Gray and Sandberg and their colleagues report the presence of three repeating sequences – a tetrapeptide, Val_1-Pro_2-Gly_3-Gly_4, a pentapeptide, Val_1-Pro_2-Gly_3-Val_4-Gly_5, and a hexapeptide, Ala_1-Pro_2-Gly_3-Val_4-Gly_5-Val_6. The repeats are listed and numbered on the basis of the conformational units to be described below. Over the past 3 years these repeats (and cyclically varied permutations), their oligomers, and high polymers have been synthesized in this laboratory and their conformations studied by spectroscopic methods with particular emphasis on evaluating their secondary structures.[35-48] The object of this article is to review this work and to include new data for the purpose of more fully achieving comparisons of the secondary structures of the three peptide systems in several solvents.

In what follows, proton and carbon-13 magnetic resonance methods of evaluating polypeptide secondary structure in solution will be briefly outlined. Then the repeat tetrapeptide, the repeat pentapeptide, and the repeat hexapeptide studies will be outlined and a final section will consider the relationships of the repeat peptides to elements of fibrous elastin.

*The work for this article was supported by the National Institutes of Health Grant number HL 11310.

II. PROTON AND CARBON-13 MAGNETIC RESONANCE EVALUATION OF POLYPEPTIDE SECONDARY STRUCTURE IN SOLUTION

Temperature* and solvent dependences of peptide NH proton and peptide carbonyl carbon (C-O) chemical shifts can be used to assess the relative exposure to the solvent or the relative shielding from the solvent of these moieties. A significant means of shielding from the solvent is by an intramolecular hydrogen bond. The observables in the NMR experiments of our immediate concern for the study of secondary structure are the chemical shift, δ, the temperature dependence of chemical shift in the i^{th} solvent, $d\delta/dT_i$, and change in chemical shift when going from the i^{th} to the j^{th} solvent system, $\Delta\delta/\Delta S_{i,j} = \delta_j - \delta_i$.

A. Complications in the Approach

Complications inherent in the approach derive from the peptide moiety itself, from the polypeptide backbone, from the side chains, and from components in the solvent. With regard to interactions with the solvent, the peptide moiety, 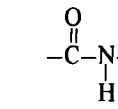 , is bifunctional. Because of this, the relative sensitivity of the chemical shift of the carbonyl carbon resonance, for example, to changes in the interactions at the oxygen end as compared to changes in interactions at the proton end of the peptide moiety, becomes of primary concern. Considering a change in state as either a change in temperature or a change in solvent system, the peptide moiety can undergo 1 of 16 different transitions during a change in state as indicated in Table 1. The special cases of no change in secondary structure during the perturbation of temperature or solvent are given by the identity transitions A1, A4, D1, and D4. If it can be argued that a given secondary structural feature does not change between two appropriate solvents and over a given temperature range, then the problem reduces to consideration of the identity transitions. Characteristic perturbation shifts for these special cases are given in Table 2. These values were derived from the model systems gramicidin S,[49] cyclohexylalanyl gramicidin S,[50] the valinomycin-K^+ complex,[49] and a series of dipeptides.[50] From studies on dipeptides, e.g., comparisons of NAc-Gly(1-C-13)-Pro-OMe with NAc-Gly(1-C-13)-Ala-OMe, of NAc-Val(1-C-13)-Pro-OMe with NAc-Val(1-C-13)-Ala-OMe, etc. in seven solvents it appears that less than 20% of a solvent elicited change in carbonyl carbon resonances occurs through the peptide NH.[50]

The complications derived from the polypeptide backbone may be considered as sequence effects, slowly interconverting states, magnetic anisotropy of vicinal peptide moieties, and *cis-trans* isomerism. The question of sequence effects (i.e., Does the peptide moiety derived from a Gly-Gly sequence respond differently from that of a Val-Pro sequence due to inductive or steric reasons?) has been answered in that the solvent shifts for an exposed C-O are similar within ±10% regardless of the sequence,[50] even though the chemical shifts in a given solvent are quite different. In conventional proton magnetic resonance studies, the problem of slowly interconverting states is seen as two resonances, the sum of which is one nucleus, that is, it is often apparent when present. The complication of the magnetic anisotropy of a vicinal group, particularly when conformation is maintained, can actually be diagnostic for a specific conformational feature, as for example has been proposed for the β-turn.[51] When average conformation is changing, magnetic anisotropy of a vicinal group can lead to fortuitously high or low values for $d\delta/dT$ and $\Delta\delta/\Delta S$.

The complications derived from side chains are shielding of the peptide moiety by hydrogen bonding or by steric effects, catalysis of peptide NH exchange, and magnetic anisotropy. The shielding of a C-O or NH moiety from the solvent by a carboxamide group, for example, is a serious complication to evaluation of polypeptide secondary structure. Catalysis of peptide NH exchange is usually detectable as an upfield shifting and a broadening of the resonance line with increasing temperature. This gives fortuitously large tempera-

*It should be appreciated that a temperature effect that does not result in a backbone conformational change is actually a comparison of the effect of temperature on solvation of an exposed moiety with a lesser effect of temperature on the vibrational state of the intramolecular hydrogen bond.

TABLE 1

Transitions in the State of Peptide Moieties During Perturbation Studies

A1	$CO_{se}\ NH_{se}$	$\longrightarrow CO_{se}\ NH_{se}$	B1	$CO_{se}\ NH_{se}$	$\longrightarrow CO_{ss}\ NH_{se}$
A2	$CO_{se}\ NH_{se}$	$\longrightarrow CO_{se}\ NH_{ss}$	B2	$CO_{se}\ NH_{se}$	$\longrightarrow CO_{ss}\ NH_{ss}$
A3	$CO_{se}\ NH_{ss}$	$\longrightarrow CO_{se}\ NH_{se}$	B3	$CO_{se}\ NH_{ss}$	$\longrightarrow CO_{ss}\ NH_{se}$
A4	$CO_{se}\ NH_{ss}$	$\longrightarrow CO_{se}\ NH_{ss}$	B4	$CO_{se}\ NH_{ss}$	$\longrightarrow CO_{ss}\ NH_{ss}$
C1	$CO_{ss}\ NH_{se}$	$\longrightarrow CO_{se}\ NH_{se}$	D1	$CO_{ss}\ NH_{se}$	$\longrightarrow CO_{ss}\ NH_{se}$
C2	$CO_{ss}\ NH_{se}$	$\longrightarrow CO_{se}\ NH_{ss}$	D2	$CO_{ss}\ NH_{se}$	$\longrightarrow CO_{ss}\ NH_{ss}$
C3	$CO_{ss}\ NH_{ss}$	$\longrightarrow CO_{se}\ NH_{se}$	D3	$CO_{ss}\ NH_{ss}$	$\longrightarrow CO_{ss}\ NH_{se}$
C4	$CO_{ss}\ NH_{ss}$	$\longrightarrow CO_{se}\ NH_{ss}$	D4	$CO_{ss}\ NH_{ss}$	$\longrightarrow CO_{ss}\ NH_{ss}$

Unique Transitions

A1	B1 = -C1	D1
A2 = -A3	B2 = -C3	D2 = -D3
A4	B3 = -C2	D4
	B4 = -C4	

se = solvent exposed ss = solvent shielded

ture coefficients, $|d\delta/dT|$, but is usually apparent, whether caused by side chain groups or other weak acids or bases in the solvent. The magnetic anisotropy of aromatic side chains can greatly complicate interpretation of C-O and NH shifts. These, however, can be clarified by hydrogenation as in conversion of a phenylalanyl residue to a cyclohexylalanyl residue, often without disrupting the polypeptide structure.[50] The substantial advantage of studying the secondary structure of the repeat elastin peptides by these methods is the absence of the above side chain complications.

B. Probability of a Given Hydrogen Bond

For rapidly interconverting states where only a single resonance is observed for each nucleus, the observable, a_{obs} – whether it be chemical shift, δ, temperature dependence of chemical, $d\delta/dT$, or solvent shift, $\Delta\delta/\Delta S$ – is given by a summation over the i states of the nucleus, i.e.,

$$a_{obs} = \sum_i \chi_i a_i, \tag{1}$$

where χ_i is the mole fraction of nuclei in the i^{th} state. Solving for χ_i gives:

$$\chi_i = \frac{a_{obs} - \left(\sum_{i \neq j} 1 + \sum_{k \neq i,j} \right) \chi_k \; a_j}{a_j - \sum_{j \neq i} a_j} \tag{2}$$

If we group the nuclei into solvent exposed, e, and solvent shielded, s, Equation 2 reduces to the familiar expression for the mole fraction in the shielded state

$$\chi_s = \frac{a_{obs} - a_e}{a_s - a_e} \tag{3}$$

For temperature studies the superscript T is used, e.g., a_s^T, and for solvent titrations giving rise to solvent shift data, the superscript st is used, e.g., a_s^{st}. This may be considered a shorthand notation for use of data in Equation 3, such as given in Table 2. For example, in a PMR temperature study,

$$a_s^T \equiv (d\delta/dT)_{A4}, \tag{4}$$

$$a_e^T \equiv (d\delta/dT)_{D1}, \tag{5}$$

where A4 defines a solvent shielded peptide NH and D1 defines a solvent exposed peptide NH as indicated in Tables 1 and 2. For a PMR solvent shift study,

$$a_s^{st} \equiv (\Delta\delta/\Delta S_{i,j})_{A4} \tag{6}$$

$$a_e^{st} \equiv (\Delta\delta/\Delta S_{i,j})_{D1}. \tag{7}$$

Because the carbonyl is the other end of the

TABLE 2

Characteristic Perturbation Shifts for Transitions of Peptide Moieties

A. PMR studies, temperature coefficients

TRANSITION	$d\delta/dT_1$[a]	$d\delta/dT_2$[a]	$d\delta/dT_3$[a]	$d\delta/dT_4$[a]
A1 $(CO_{se}NH_{se})$[c]	-5.3	-7.5	-7.6	-
A4 $(CO_{se}NH_{ss})$[d]	-3.4	-3.0	-4	-4.5
D1 $(CO_{ss}NH_{se})$[d]	-8.0	-7.5	-8	-9
D4 $(CO_{ss}NH_{ss})$[e]	-	-2	-2	-

B. PMR studies, solvent shifts

TRANSITION	$\Delta\delta/\Delta S_{1,3}$[b]	$\Delta\delta/\Delta S_{2,3}$[b]	$\Delta\delta/\Delta S_{3,4}$[b]
A1 $(CO_{se}NH_{se})$[c]	-0.84	-0.97	-
A4 $(CO_{se}NH_{ss})$[d]	0.60	0.15	0.24
D1 $(CO_{ss}NH_{se})$[d]	-1.10	-1.00	0.74
D4 $(CO_{ss}NH_{ss})$[e]	-	0.0	-

C. CMR studies, solvent shifts

TRANSITION	$\Delta\delta/\Delta S_{1,2}$[b]	$\Delta\delta_{mi}$[f]	$\Delta\delta/\Delta S_{1,3}$[b]	$\Delta\delta_{mi}$[f]	$\Delta\delta/\Delta S_{1,4}$[b]	$\Delta\delta_{mi}$[f]
A1 $(CO_{se}NH_{se})$[c]	2.5		3.2		-	
A4 $(CO_{se}NH_{ss})$[d]	2.5	0.7	3.5	1.1	4.0	1.0
D1 $(CO_{ss}NH_{se})$[d]	1.8	0	2.4	0	3.0	0
D4 $(CO_{ss}NH_{ss})$[e]	-		-		-	

[a] $d\delta/dT_i$ is the temperature coefficient for chemical shift given in ppm/deg × 10^3 for the i^{th} solvent, also given in the text where $a_e^T = d\delta/dT$ for D1 and $a_s^T = d\delta/dT$ for A4. The solvents are (1) Me_2SO-d_6, (2) MeOH, (3) CF_3CH_2OH, and (4) H_2O.

[b] $\Delta\delta/\Delta S_{i,j}$ is the solvent shift in ppm for going from solvent i to solvent j as defined in Tables 2 and 3, also given in the text where $a_e^{st} = \Delta\delta/\Delta S$ for D1 and $a_s^{st} = \Delta\delta/\Delta S$ for A4. The solvents for the CMR studies are (1) Me_2SO-d_6, (2) CD_3OD, (3) CF_3CD_2OD, and (4) D_2O.

[c] The values for A1 were approximated from dipeptide data. Actually there appears to be substantial shielding of the NH in solvent 1.

[d] The values for A4 and D1 were estimated from gramicidin S and Cha gramicidin S.[49,50]

[e] The values for D4 were obtained from the valinomycin-K^+ complex.[49]

[f] $\Delta\delta_{mi}$ defined in Table 6.

peptide moiety, the subscripts are exchanged in a CMR solvent shift study, i.e.,

$$a_s^{st} \equiv (\Delta\delta/\Delta S_{i,j})_{D1}, \quad (8)$$

$$a_e^{st} \equiv (\Delta\delta/\Delta S_{i,j})_{A4}. \quad (9)$$

Until more information on model systems is available to complete the data for all the transitions indicated in Table 1, we will cautiously use the values in Table 2 for solvent exposed and solvent shielded moieties recognizing that a significant effect on NH solvent shift can arise from interaction at the C-O of the same peptide moiety. It is quite possible that $d\delta/dT$ for a peptide NH is not highly dependent on whether the associated C-O is solvent shielded or solvent exposed. At this stage, however, a calculated mole fraction of peptide NH shielding should be considered only in a grossly qualitative sense. The shielding of the peptide C-O moiety is at an even more qualitative stage.

III. THE REPEAT TETRAPEPTIDE OF ELASTIN

Conformational studies on the repeat tetrapeptide of elastin have been based on a host of synthetic peptides. The following are a few: $(VPGG)_n$* where n = 1, 2, 3, and 4; HCO-$(VPGG)_n$-V-OMe where in three different syntheses n has been approximated as 8, 40, and 35; $(PGGV)_n$ where n = 1, 3, and 4 and the cyclic analogs for n = 3 and 4; the cyclododeca- and the cyclohexadecapeptides. Variations have also been carried out on the end groups. Selected N-methyl residues have been incorporated to check assignments and proposed conformational features, and selected isotope enrichment has been utilized to achieve unambiguous resonance assignments.

A. Proton Magnetic Resonance[36,38]

Complete proton magnetic resonance (PMR) spectra at 20°C and 99°C in Me_2SO-d_6 are given in Figure 1 for the polytetrapeptide, HCO-(Val_1-Pro_2-Gly_3-Gly_4)$_n$-Val-OMe, where the average value of n is approximately 35. The resonances are seen to be fairly broad due to the size of the polymer. All assignments are indicated; they are based initially on the monomer and the oligomers.

1. Temperature Dependence of Peptide NH Chemical Shifts

Detailed temperature studies have been carried out in four solvents: Me_2SO-d_6, methanol, trifluoroethanol, and water. Plots of the peptide NH chemical shifts as a function of temperature are reported in Figure 2. What is immediately apparent in Figure 2 is the similarity of the temperature dependences in methanol and in water up to 50°C (compare Figures 2B and 2D). In both solvents the Gly_4 NH exhibits the lesser temperature dependence. The Gly_4 NH also exhibits the lowest temperature coefficient in Me_2SO-d_6. Qualitatively in the three solvents Me_2SO-d_6, MeOH, and H_2O, the Gly_4 NH appears to be relatively shielded from the solvent and the Val_1 NH and Gly_3 NH protons appear to be relatively more solvent exposed. In trifluoroethanol the situation appears quite different for the polytetrapeptide where it is the Val_1 NH that exhibits the lesser temperature coefficient. The temperature coefficients and 0°C intercepts are tabulated for each peptide NH in Table 3 for each of the four solvents and for two temperature ranges 0 to 50°C and 50 to 100°C in water.

The most immediate concern in utilizing the data of Figure 2 is to determine the basis for the shielding of the Gly_4 NH in dimethyl sulfoxide, methanol, and water. This may be done by studying the monomer, $V_1P_2G_3G_4$, a permutation of the monomer, $P_2G_3G_4V_1$, and an oligomer, $H(P_2G_3G_4V_1)_3OH$. Shielding is observed in methanol for Boc $V_1P_2G_3G_4$-OMe where the Gly_4 NH exhibits one half the slope of the Gly_3 NH, whereas no shielding is observed with H $P_2G_3G_4V_1$-OMe. This suggests that the Val_1 C-O, which would be required to form a ten-atom hydrogen bonded ring, referred to as a β-turn, is the source of shielding. A temperature study of the peptide $H(P_2G_3G_4V_1)_3OH$ in methanol shows two Gly_4 NH protons to be upfield with 0°C intercepts at 8.42 ppm and with temperature coefficients of 3×10^{-3} ppm/deg. Three Gly_3 NH protons are at lower field, 0°C intercepts at 8.72 ppm with a $d\delta/dT_2$ of 7×10^{-3} ppm/deg (these values may be compared with those given in Table 3 for methanol). A single triplet, the Gly_4 NH of the initial repeat, has a 0°C intercept at 8.68 ppm and a slope of 5.2×10^{-3} ppm/deg. The conclusion is that the Gly_4 NH protons of the second

*The following one letter abbreviations will be used: V = Val, P = Pro, G = Gly, A = Ala.

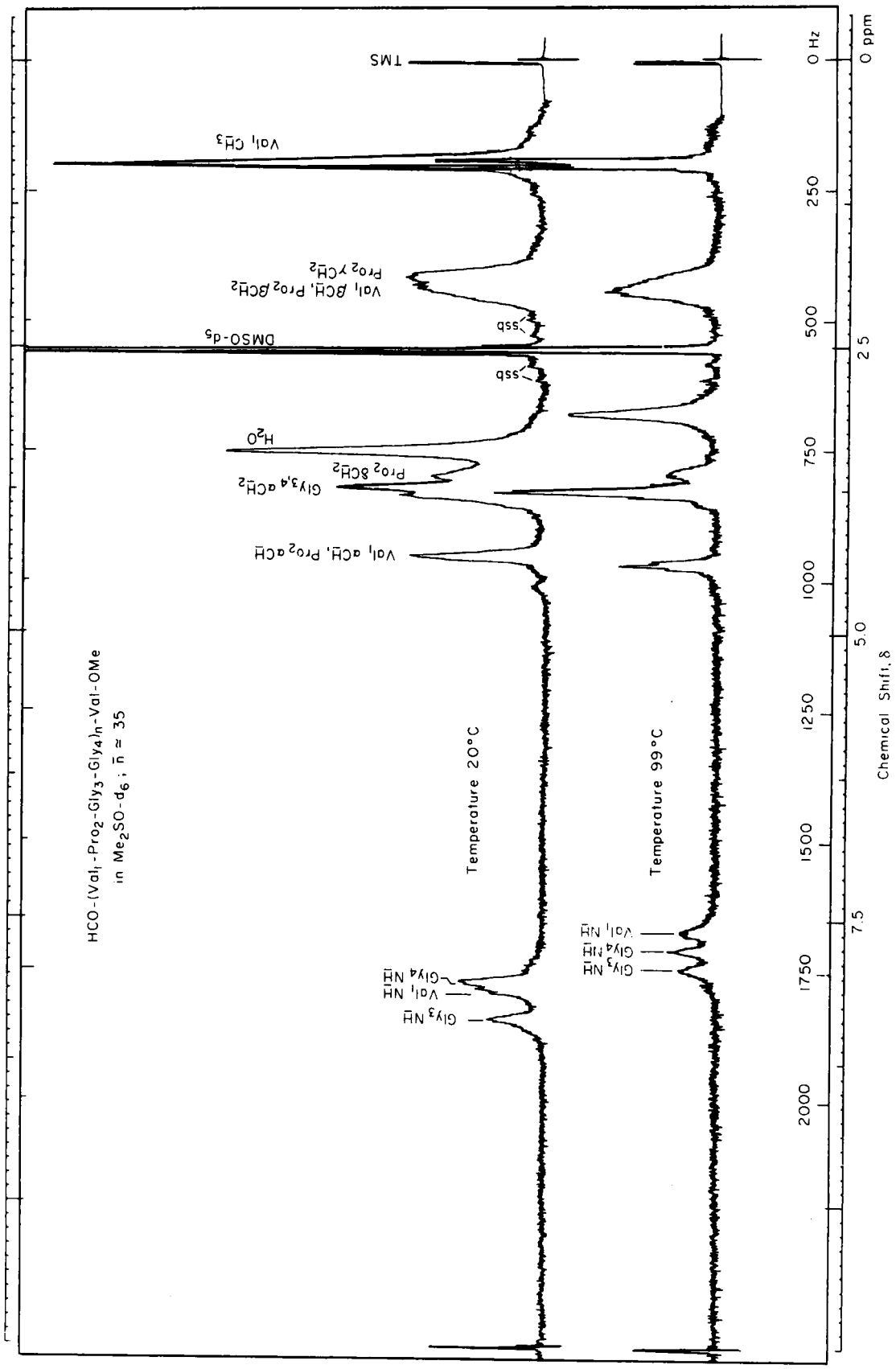

FIGURE 1. Proton magnetic resonance spectrum of HCO-(Val_1-Pro_2-Gly_3-Gly_4)$_n$-Val-OMe in dimethyl sulfoxide.

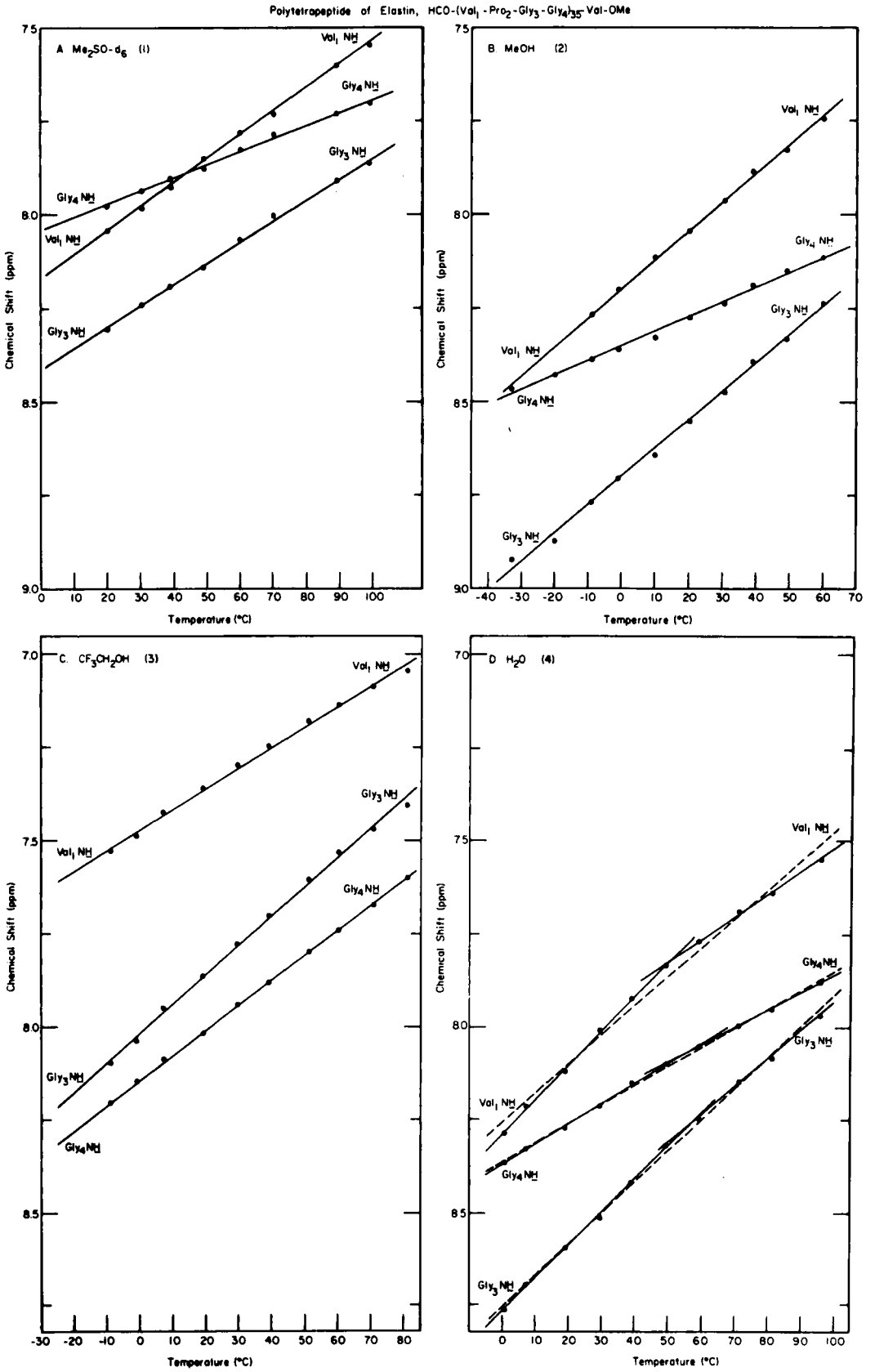

FIGURE 2. Temperature dependence of the proton chemical shift of HCO-(Val$_1$-Pro$_2$-Gly$_3$-Gly$_4$)$_n$-Val-OMe in dimethyl sulfoxide, methanol, trifluoroethanol, and water.

TABLE 3

Temperature Dependence of Peptide NH Chemical Shifts of HCO-(Val_1-Pro_2-Gly_3-Gly_4)$_{3,5}$-Val-OMe in Several Solvents

PEPTIDE	Me_2SO-d_6		MeOH		CF_3CH_2OH		H_2O(0-50°C)		H_2O(50-100°C)	
RESIDUE	$d\delta/dT_1$[a]	0°/Intercept	$d\delta/dT_2$[a]	0°/Intercept	$d\delta/dT_3$[a]	0°/Intercept	$d\delta/dT_4$[a]	0°/Intercept	$d\delta/dT_4$[a]	0°/Intercept
Val_1 NH	-6.4	8.17	-7.7	8.20	-5.6	7.47	-9.2	8.28	-6.2	8.13
Gly_3 NH	-5.6	8.41	-7.6	8.70	-7.9	8.02	-8.9	8.76	-7.6	8.68
Gly_4 NH	-3.5	8.04	-4.0	8.35	-6.7	8.14	-5.5	8.36	-4.7	8.32

[a]Multiply by 10^{-3} to obtain coefficients in ppm/degree; multiply by 2.2 for Hz/10°C at 220 MHz.

TABLE 4

Calculated Mole Fractions of Shielding for HCO-(Val_1-Pro_2-Gly_3-Gly_4)$_{3.5}$-Val-OMe Based on Temperature Studies

PEPTIDE RESIDUE	Me_2SO-d_6	MeOH	CF_3CH_2OH	H_2O (0-50°C)	H_2O (50-100°C)
x_S^T (Val_1 NH)	0.35	0	0.60	0	0.64
x_S^T (Gly_3 NH)	0.52	0.02	0.03	0.06	0.34
x_S^T (Gly_4 NH)	0.98	0.79	0.33	0.71	0.86

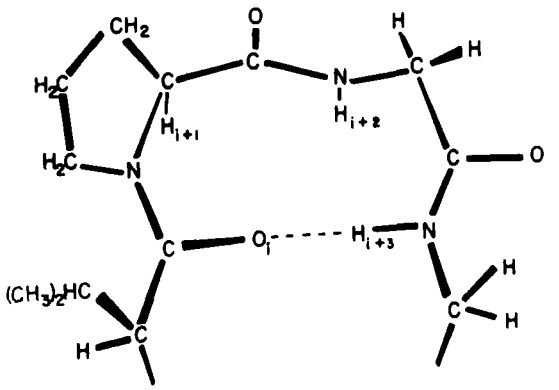

FIGURE 3. Proposed β-turn for the repeating tetrapeptide Val_1-Pro_2-Gly_3-Gly_4. (From Urry, D. W. and Ohnishi, T., *Biopolymers*, 13, 1223, 1974. With permission.)

and third repeats are upfield and shielded whereas the Gly_4 NH of the initial repeat of $H(P_2G_3G_4V_1)_3$-OH is downfield and more solvent exposed. The implication is that the Val_1 C-O is required for shielding by the formation of a β-turn (see Figure 3), and that the NH which is involved in the hydrogen bond of the β-turn is characteristically at higher field.[51] A similar β-turn with Pro as residue i + 1 and Gly as i + 2 was suggested to be the most stable conformational feature of cyclo $(PGG)_2$ by Pease et al.[52]

Having established that the shielding of the Gly_4 NH is due to intramolecular hydrogen bonding, it is of interest to obtain an approximate value for the probability of formation of the hydrogen bond, i.e., to calculate a value for the mole fraction of shielding. Utilizing the temperature coefficients $d\delta/dT_i$ of Table 2 in Equation 3 with the identities of Equations 4 and 5 and the observed values for the peptide NH chemical shifts of the polytetrapeptide given in Table 3, the calculated mole fractions of shielding for each peptide NH in each solvent are listed in Table 4. These values can be used to obtain a qualitative view of the β-turn of Figure 3 as a conformational feature of the polytetrapeptides and to assess solvent dependence.

A striking feature of Table 4 is the similarity of the shielding pattern in methanol and water (0 to 50°C), where only the Gly_4 NH is seen as shielded. In methanol and presumably in water (0 to 50°C), the only significant conformational feature is the β-turn of Figure 3. In dimethyl sulfoxide, while the shielding of the Gly_4 NH appears to be complete, the other peptide NHs exhibit significant shielding. It is clear from both Figure 2 and Table 4 that the β-turn of Figure 3 is not the dominant conformational feature in trifluoroethanol where the Val_1 NH appears to be the most shielded. Water presents an interesting case where an abrupt change in slope occurs at 50°C (see Figure 2D). This is a clear demonstration of a change in average conformation with increasing temperature where the most prominent change is the increased shielding of the Val_1 NH.

2. Solvent Dependence of Peptide NH Chemical Shifts

In order to use most effectively a solvent shift to assess peptide NH exposure to solvent, it is necessary that the conformation be the same in both solvents. The preferred solvent pairs for obtaining a solvent shift which can be related to shielding from the solvent involve trifluoroethanol. In this regard the situation for the polytetrapeptide is complicated by the obviously different conformation in trifluoroethanol as seen in Table 4. The values for the chemical shifts at 20°C for the polytetrapeptide NH resonances as well as the calculated solvent shifts for several solvent pairs are listed in Table 5. Noting the solvent shifts

TABLE 5

Solvent Dependence of HCO-(Val_1-Pro_2-Gly_3-Gly_4)$_{3,5}$-Val-OMe Peptide NH Chemical Shifts at 20°C

PEPTIDE RESIDUE	1 Me_2SO-d_6	2 MeOH	3 $CF_3CH_2^iOH$	4 H_2O	$\Delta\delta/\Delta_{1,3}$	$\Delta\delta/\Delta S_{2,3}$	$\Delta\delta/\Delta S_{3,4}$
Val_1 NH	8.04	8.05	7.36	8.10	-0.68	-0.69	0.74
Gly_3 NH	8.30	8.55	7.86	8.58	-0.44	-0.69	0.72
Gly_4 NH	7.97	8.27	8.01	8.25	-0.04	-0.26	0.24

listed for the Me_2SO-d_6–CF_3CH_2OH (1,3) and methanol-trifluoroethanol (2,3) solvent pairs, it is the Gly_4 NH which shows the smallest solvent shift and the most apparent shielding from the solvent. While the above mentioned limitation must be kept in mind, Figure 4 shows that the Gly_4 NH still is qualitatively delineated. A similar delineation is seen for the trifluoroethanol – water (3,4) solvent pair (see Table 5). The reason for this delineation could be a result of the high-field shifted position of the Gly_4 NH resonance when in the β-turn of Figure 3, which has been suggested as arising from the magnetic anisotropy of the carbonyl moiety of residue i + 1.[51] The reasoning is that disruption of the β-turn results in a downfield shift which largely offsets the upfield shift that trifluoroethanol exerts on solvent exposed peptide NH protons. Alternatively this β-turn may be substantially retained and additional features added in trifluoroethanol and at elevated temperatures in water as well as in dimethyl sulfoxide.

B. Carbon-13 Magnetic Resonance[42,43]

The complete carbon-13 magnetic resonance (CMR) spectrum of the polytetrapeptide in D_2O is given in Figure 5. Assignments of all resonances were made by stepwise buildup of the repeating unit and by varying end groups and, in addition for the carbonyl carbon resonances, by 1-C-13 enrichment.[43]

1. Solvent Dependence of Peptide Carbonyl Carbon Chemical Shifts

The basic idea behind utilization of CMR for the evaluation of polypeptide secondary structure is that the resonance position of the exposed carbonyl carbon exhibits large downfield shifts on going from a nonproton-donating solvent to a proton-donating solvent whereas the resonance of an intramolecularly hydrogen bonded carbonyl moiety does not undergo such a large downfield shift, partly because it is already shifted somewhat downfield by the peptide NH to which it is hydrogen bonded. A good nonproton donating solvent for polypeptides is dimethyl sulfoxide, whereas all three, methanol, trifluoroethanol, and water, are good proton-donating solvents. The solvent perturbation approach in the CMR, as with the PMR, is applied most readily when there is good evidence that little or no conformational change occurs on changing solvent.

Chemical shifts for the carbonyl carbon resonances are listed in Table 6 as well as the solvent shifts for the solvent pairs Me_2So-d_6 – CD_3OD (1→2), Me_2SO-d_6 – CF_3CD_2OD (1→3), and Me_2SO-d_6 – D_2O (1→4). The solvent titrations for two of these solvent pairs are given in Figure 6A and 6B. The Val_1 C-O shows the least downfield shift in each of the three titrations and is used as the internal reference in the column labeled $\Delta\delta_{ml}$. The Gly_4 C-O is the next most solvent shielded followed by the Pro_2 C-O. The Gly_3 C-O is the most solvent exposed. The situation is similar in each of the solvent pairs with only minor variation. The similarity of the patterns for each of the solvent pairs may be because they largely reflect the conformation in Me_2SO-d_6. With this in mind it is interesting to begin to pair, on the basis of relative shielding, these delineated C-O resonances with the delineated peptide NH resonances as tabulated in Table 6 in terms of the mole fraction of shielding for the 1→4 solvent shift. Taking the Gly_3 C-O as being completely exposed and the Val_1 C-O as being completely shielded, the denominator of Equation 3 becomes - 1.02 and the numerators are 0 - 1.02 for the Val_1 C-O, 0.8 - 1.02 for the Pro_2 C-O, 1.02 to 1.02 for the Gly_3 C-O, and 0.46 - 1.02 for the Gly_4 C-O, that is, $a_s^{st} = 0$, $a_e^{st} = 1.02$. This gives:

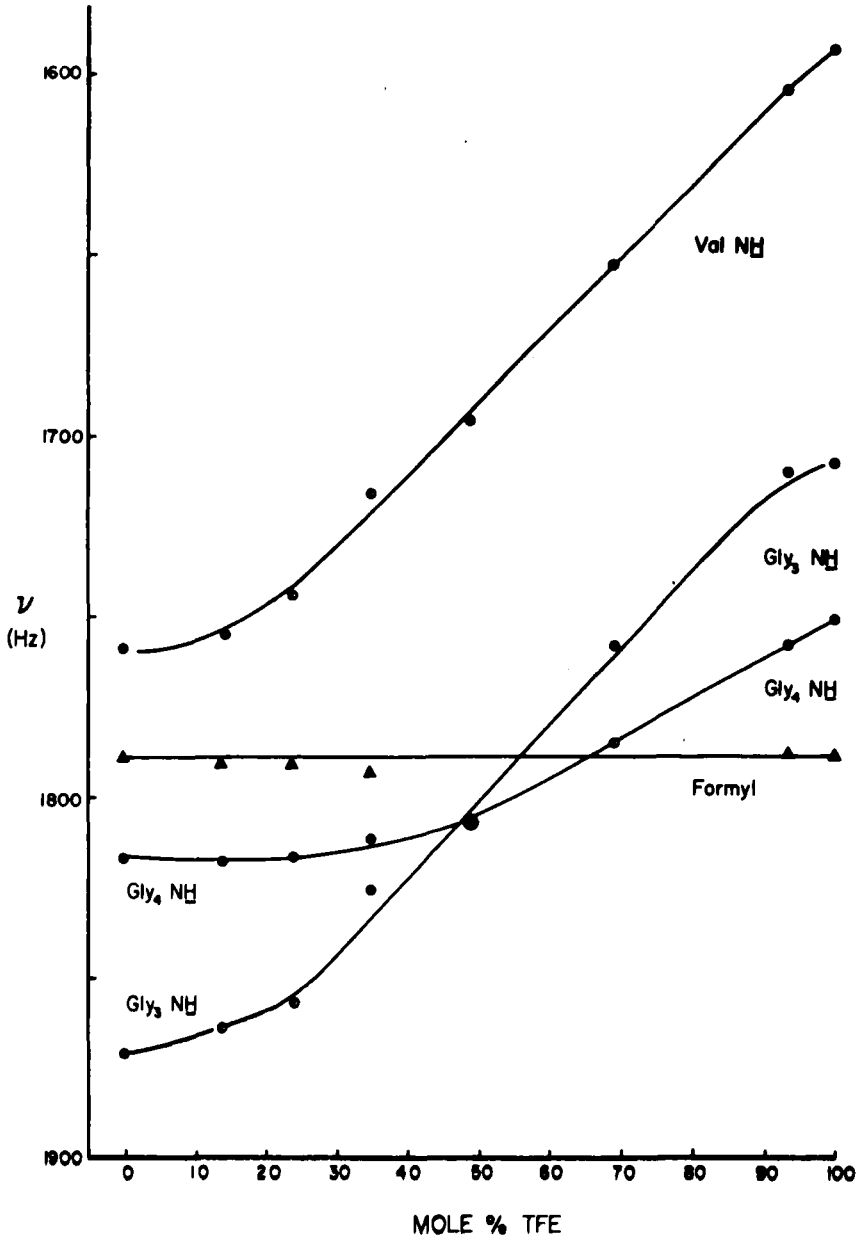

FIGURE 4. Methanol-trifluoroethanol solvent-mixture dependence of chemical shift for HCO-(Val_1-Pro_2-Gly_3 Gly_4)$_{4\,0}$-Val-OMe. (Adapted from Urry, D. W. and Ohnishi, *T., Biopolymers, 13, 1223, 1974.)*

$$\chi_s^{st}(Val_1\ \underline{C}\text{-}O) = 1.0 \quad \chi_s^{st}(Pro_2\ \underline{C}\text{-}O) = 0.22$$
$$\chi_s^{st}(Gly_3\ \underline{C}\text{-}O) = 0 \quad \chi_s^{st}(Gly_4\ \underline{C}\text{-}O) = 0.55. \qquad (10)$$

On the basis of mole fraction of shielding the Val_1 C-O pairs with the Gly_4 NH (1.0 and 0.98), the Pro_2 C-O pairs with the Val_1 NH (0.22 and 0.35), and the Gly_4 C-O pairs with the Gly_3 NH (0.55 and 0.52). Interestingly, these could all be β-turns, ten-atom hydrogen bonded rings, which are the most obvious pairings. More complex sets of conformers could give similar shieldings and it should be appreciated that shielding may not

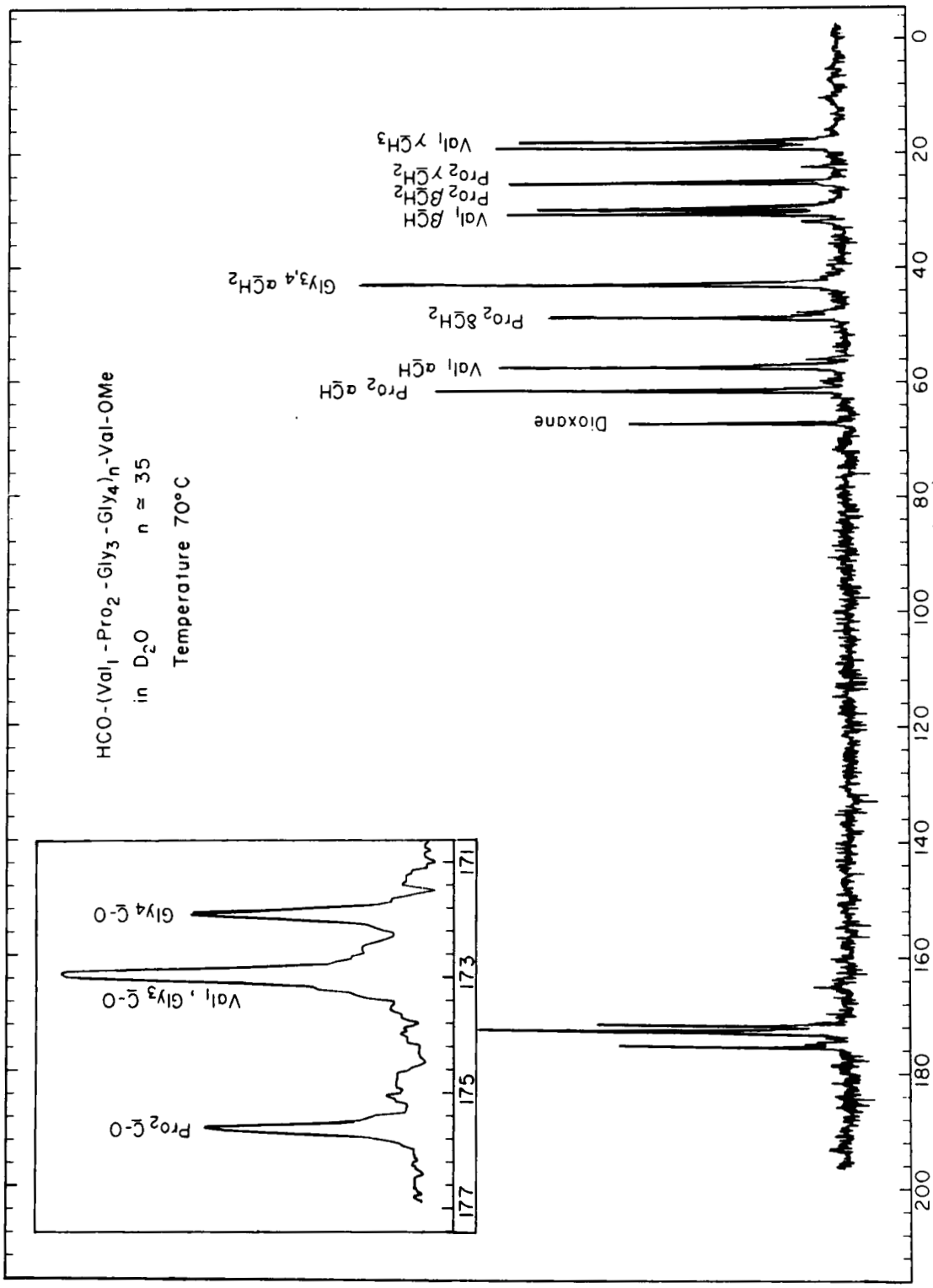

FIGURE 5. Carbon-13 magnetic resonance spectrum of HCO-(Val_1-Pro_2-Gly_3-Gly_4)$_n$-Val-OMe in D_2O.

TABLE 6

Solvent Dependence of HCO-(Val_1-Pro_2-Gly_3-Gly_4)$_n$-Val-OMe Peptide Carbonyl Chemical Shifts[a]

PEPTIDE	1	2	3	4	1 → 2		1 → 3		1 → 4	
RESIDUE	Me_2SO-d_6	CD_3OD	CF_3CD_2OD	D_2O	$\Delta\delta/\Delta S_{1,2}$	$\Delta\delta_{m1}$[b]	$\Delta\delta/\Delta S_{1,3}$	$\Delta\delta_{m1}$[b]	$\Delta\delta/\Delta S_{1,4}$	$\Delta\delta_{m1}$[b]
Val_1 C-O	169.88	172.40	173.42	172.87	2.52	0	3.59	0	2.99	0
Pro_2 C-O	171.82	174.79	175.66	175.61	2.97	0.45	3.84	0.25	3.79	0.80
Gly_3 C-O	168.86	172.01	173.33	172.87	3.15	0.63	4.47	0.88	4.01	1.02
Gly_4 C-O	168.28	171.19	172.07	171.73	2.91	0.39	3.79	0.20	3.45	0.46

[a]Adapted from Urry, D. W., Mitchell, L. W., and Ohnishi, T., *Biochem. Biophys. Res. Commun.*, 59, 62, 1974.
[b]$\Delta\delta_{m1} = (\Delta\delta/\Delta S_{i,j})_m - (\Delta\delta/\Delta S_{i,j})_1$ where m stands for the m^{th} residue and 1 for residue 1, that is, the residue 1 carbonyl carbon resonance is used as an internal reference. Residue 1 was chosen as it exhibited the least solvent dependence.

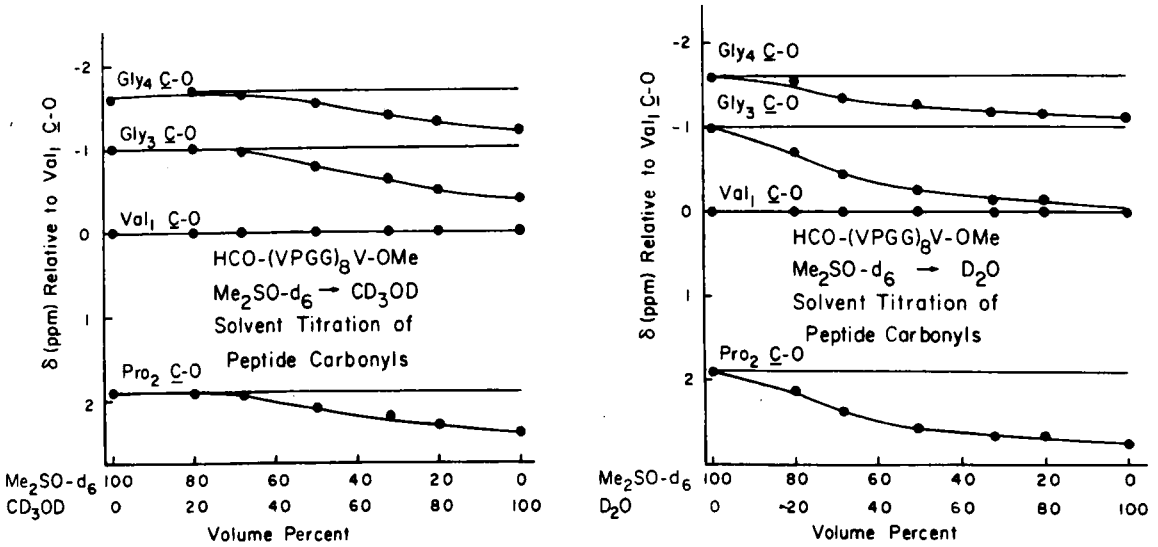

FIGURE 6. Dimethyl sulfoxide to methanol (A) and dimethyl sulfoxide to water (B) solvent titrations of the peptide carbonyls of the tetramer high polymer. (From Urry, D. W., Mitchell, L. W., and Ohnishi, T., *Biochem. Biophys. Res. Commun.*, 59, 62, 1974. With permission.)

always be due to an intramolecular hydrogen bond.

C. Proposed Conformations for Each Solvent

On the basis of the PMR data alone, the β-turn in Figure 3 was proposed and strongly supported for methanol, that is, the shielding from solvent of the Gly_4 NH required the Val_1 C-O immediately preceding it in the sequence. One can also argue independently from the CMR data that shielding from solvent of the Val_1 C-O requires the Gly_4 NH following it in the sequence.[42] In a Me_2SO-d_6 → CD_3OD solvent shift study of the tripeptide HCO-Val_1-Pro_2-Gly_3-OMe, the Val_1 C-O and Pro_2 C-O exhibit identical solvent shifts whereas using the same solvent pair for the tetrapeptide, HCO-Val_1-Pro_2-Gly_3-Gly_4-OMe, the Pro_2 C-O shifts further downfield than the Val_1 C-O by 0.58 ppm. The interpretation is that the Gly_4 NH shields the Val_1 C-O. Thus, independently by PMR and CMR one concludes the presence of the $Val_{1,i}$ C-O · · · HN $Gly_{4,i}$ β-turn of Figure 3 for both dimethyl sulfoxide and methanol. Also the similarity of the temperature dependence curves in methanol and H_2O (0 to 50°C) in Figure 2 suggests the same conformational feature in water below 50°C.

Additional secondary structural features are suggested by the data as occurring with less probability. For the moment, if we consider the most obvious pairings noted above for dimethyl sulfoxide a second ten-atom hydrogen bonded ring, $Gly_{4,i-1}$ C-O · · · HN $Gly_{3,i}$, would occur about 50% of the time and a third ten-atom hydrogen bonded ring, $Pro_{2,i}$ C-O · · · HN $Val_{1,i+1}$, would occur about 30% of the time on the basis of the χ_s^T values. Changing solvents would alter the probability of these hydrogen bonds. If all three hydrogen bonds as indicated in Figure 7A were to occur simultaneously, the structure would be approximated as turns of a 3_{10} helix disrupted by the regular occurrence of the prolyl residue.

The second ten-atom hydrogen bonded ring, $Gly_{4,i-1}$ C-O · · HN $Gly_{3,i}$, however, places L-Val-L-Pro at the corners as residues i + 1 and i + 2, respectively, of a β-turn and as such is not generally viewed as a favorable β-turn. Because of this, an alternate hydrogen bonding pattern should be considered for the shielding of the Gly_4 C-O. In the Me_2SO-d_6 → D_2O carbonyl carbon solvent shift study, the observed shifts calculated to give a mole fraction of shielding of 0.55 for the Gly_4 C-O and in water at elevated temperatures χ_s^T (Val_1 NH) = 0.64 (see Table 4). This raises the possibility of a $Gly_{4,i}$ C-O · · · HN $Val_{1,i}$ hydrogen bond. The result is a cross-β-structure as indicated in Figure 7C. There are several reasons why this cross-β-structure requires consideration.

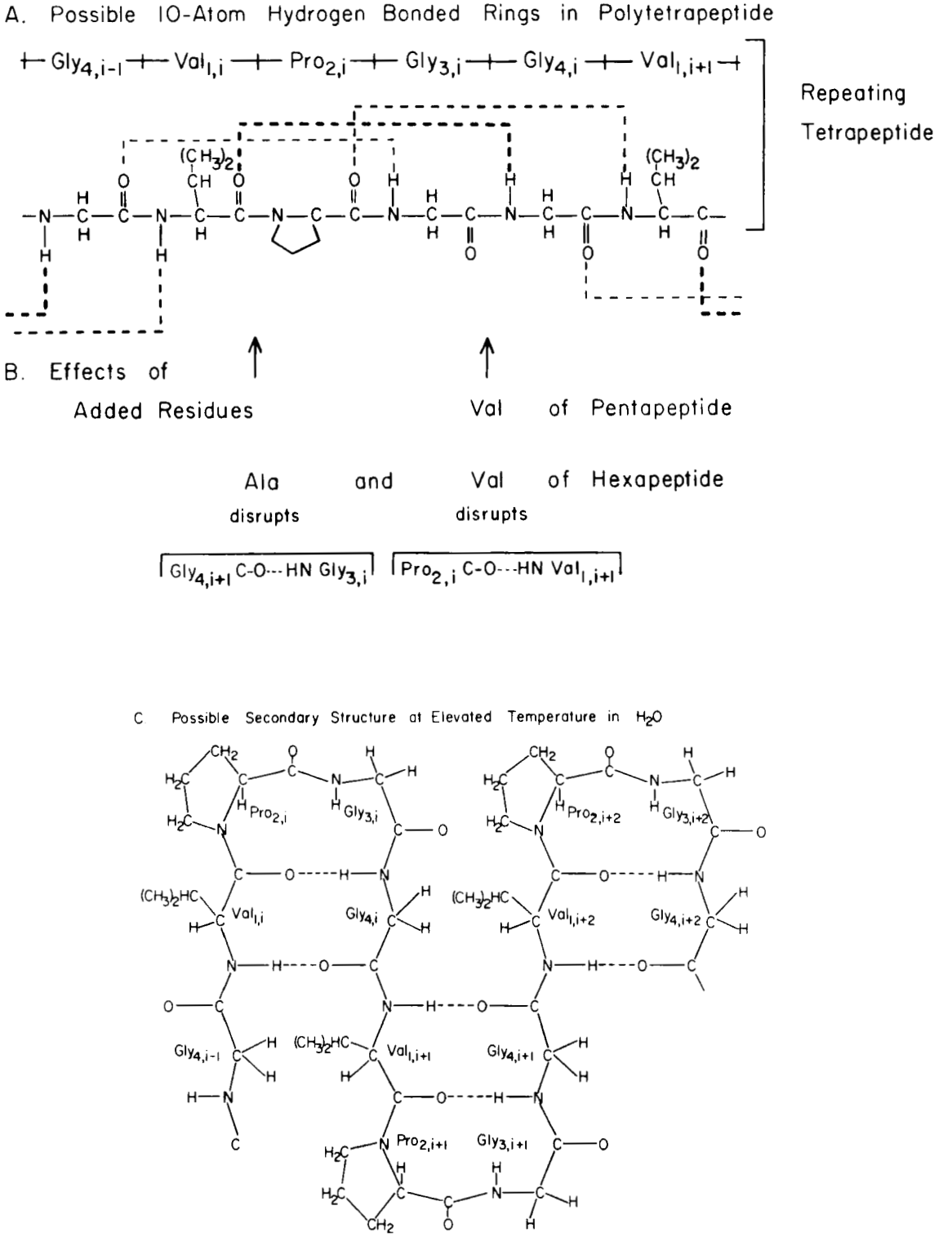

FIGURE 7. Ten-atom hydrogen bonded rings of the tetramer high polymer.

Firstly, with the β-turns tilted in a louvered arrangement, some intramolecular hydrophobic association can occur which would be consistent with the apparent transition to a state of greater order on raising the temperature in water. Secondly, a hyperchromism is observed when raising the temperature in water. This is consistent with the formation of a cross-β-structure. Thirdly, the polypentapeptide also shows a correlated increase in shielding of residue$_1$ NH and the residue$_4$ C-O (see below). Also the louvered effect completely exposes the Gly$_3$ C-O but causes some steric shielding of the Pro$_2$ C-O and Gly$_3$ NH.

IV. THE REPEAT PENTAPEPTIDE OF ELASTIN

In the pentapeptide series, the monomer (VPGVG), the decapeptide and pentadecapeptide oligomers, and high polymers with average values of n ranging from 15 to greater than 20 have been synthesized and studied by spectroscopic methods for the purpose of determining their conformations in solution. The following will briefly review studies primarily on the monomer and high polymer.

A. The Monomers, HCO and Boc-Val$_1$-Pro$_2$-Gly$_3$-Val$_4$-Gly$_5$-OMe[37,41,43]

The complete PMR spectrum of Boc-VPGVG-OMe is given in Figure 8 with all the resonance assignments indicated. The peptide NH protons were assigned by their splitting patterns and by chemical methods. The two doublets are Val NH resonances and the two triplets are Gly NH resonances. The Boc derivative shifts the Val$_1$ NH doublet upfield and the methyl ester shifts the Gly$_5$ NH triplet downfield. This allows assignment of the two Val NH doublets and the two Gly NH triplets. Also included in Figure 8 are decoupling experiments. For example, irradiation of the αCH protons at 875 Hz (ω_2) causes collapse of the Val$_1$ NH doublet allowing assignment of the Val αCH resonance. This is continued for four of the αCH protons and the fifth which causes no collapse of a peptide NH multiplet is the Pro αCH resonance. The very small hump very near 1,000 Hz downfield from the assigned Pro αCH resonance is a trace of the *cis* Pro isomer.

The temperature dependences of the peptide NH protons of HCO-VPGVG-OMe are given in Table 7 where the Val$_4$ NH is consistently observed to have the lowest temperature coefficient. The solvent shifts of the peptide NH protons at 20°C are listed in Table 8 where again the Val$_4$ NH is distinguished as the most shielded peptide NH (compare with characteristic values given in Table 2B). In all solvents the Val$_4$ NH is at highest field. This high field position in Me_2SO-d_6, MeOH, and H_2O is characteristic of β-turns[51] and leads to the proposal of a β-turn similar to that proposed for the tetrapeptide in Figure 3. The proposed β-turn for the pentapeptide (see Figure 9) has an identical ten-atom hydrogen bonded ring as for the tetrapeptide. The only difference is the R group of residue 4.

A CMR spectrum containing all the resonances of HCO-VPGVG-OMe is seen in Figure 10. The assignments were achieved by comparison with data on the appropriate dipeptides, tripeptides, and the tetrapeptide for the upfield resonances (< 60 ppm), by chemical modification of end residues, and enrichment for the carbonyl carbon resonances.[43] The Gly C-O resonances which overlap in this pentamer in methanol were C-13 enriched, the Gly$_3$ C-O, to 2%, and the Gly$_5$ C-O to 3%. Natural abundance of C-13 is 1.1%. This enrichment in combination with the other carbonyl carbon assignments allows these resonances to be followed throughout a solvent titration such as the Me_2SO-d_6 → D_2O titration plotted in Figure 11. The Gly$_5$ C-O is not plotted as it is the carbonyl of an ester in this pentapeptide and has a different solvent behavior than a peptide carbonyl.[43] In Figure 11 the Val$_1$ C-O is seen to exhibit the least downfield solvent shift with the Pro$_2$ C-O the most, followed by the Gly$_3$ C-O, and then the Val$_4$ C-O. The Val$_1$ C-O is, of course, the carbonyl involved in the proposed β-turn of Figure 9. The CMR results on the pentamer, therefore, substantiate the PMR conclusions and continue with the same conformational feature as in the tetramer.

It should also be noted that a partial shielding of the Gly NH protons is apparent in Table 7. In Me_2SO-d_6, in particular, the Gly$_3$ NH proton is as shielded as the Val$_4$ NH proton. Whether this derives from the formyl carbonyl in analogy to the ten-atom hydrogen bonded ring considered for this peptide NH in the tetramer where only fractional shielding was observed, or whether it may be shielded by the Gly$_5$ C-O is an important question

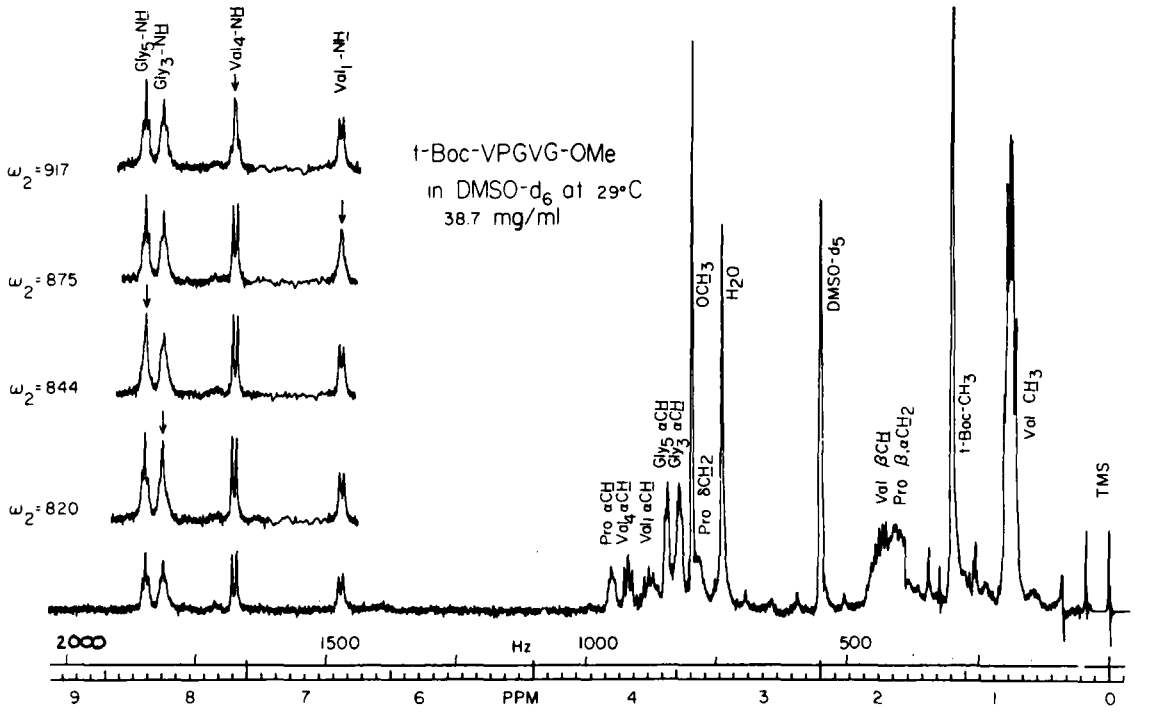

FIGURE 8. Proton magnetic resonance spectra of t-Boc-Val-Pro-Gly-Val-Gly-OMe at 220 MHz and at 29°C in dimethyl-d_6 sulfoxide. Tetramethylsilane (TMS) was used as an internal standard. All proton resonances are assigned. Also included are typical double resonance experiments which demonstrate the clarity of the decoupling experiments and serve also to provide assignments for the α-CH protons. (From Urry, D. W., Cunningham, W. D., and Ohnishi, T., *Biochemistry*, 13, 609, 1974. With permission.)

TABLE 7

Temperature Dependence of HCO-Val_1-Pro_2-Gly_3-Val_4-Gly_5-OMe Peptide NH Chemical Shifts

PEPTIDE	Me_2SO-d_5		MeOH		CF_3CH_2OH		H_2O	
RESIDUE	$d\delta/dT_1$[a]	0^o/Intercept	$d\delta/dT_2$[a]	0^o/Intercept	$d\delta/dT_3$[a]	0^o/Intercept	$d\delta/dT_4$[a]	0^o/Intercept
Val_1 NH	-6.6	8.44	-8.6	8.57	-11.4	8.01	-9.0	8.57
Gly_3 NH	-4.7	8.32	-7.5	8.60	-8.4	7.99	-8.1	8.68
Val_4 NH	-4.7	7.74	-4.8	7.98	-5.7	7.89	-7.3	8.14
Gly_5 NH	-6.6	8.60	-7.9	8.71	-8.4	7.99	-8.1	8.76

[a]Multiply by 10^{-3} to obtain coefficients in units of ppm/deg.

to resolve. The partial shielding of the Val_4 C-O in Figure 11 would not seem to be a good match for the Gly_3 NH in Me_2SO-d_6 and it is, of course, not possible for the Val_4 C-O partially to shield the Gly_5 NH as they are part of the same peptide moiety. This will be considered in greater detail below in discussion of the polypentapeptide data and will draw from hexamer data which adds a Val residue to the carboxyl end providing a Gly_5 peptide carbonyl (see Figure 20 and Tables 13 to 16).

B. The Polypentapeptide, HCO-(Val_1-Pro_2-Gly_3-Val_4-Gly_5)$_{18}$-Val-OMe[48]

1. Proton Magnetic Resonance Studies

The complete PMR spectrum of the poly-

TABLE 8

Solvent Dependence of HCO-Val_1-Pro_2-Gly_3-Val_4-Gly_5-OMe Peptide NH Chemical Shifts at 20°C

PEPTIDE RESIDUE	1 Me_2SO-d_6	2 MeOH	3 CF_3CH_2OH	4 H_2O	$\Delta\delta/\Delta S_{1,3}$	$\Delta\delta/\Delta S_{2,3}$	$\Delta\delta/\Delta S_{3,4}$
Val_1 NH	8.31	8.40	7.78	8.39	-0.53	-0.62	0.61
Gly_3 NH	8.23	8.45	7.82	8.52	-0.41	-0.63	0.70
Val_4 NH	7.65	7.88	7.78	7.99	0.13	-0.10	0.21
Gly_5 NH	8.47	8.55	7.78	8.60	-0.69	-0.77	0.82

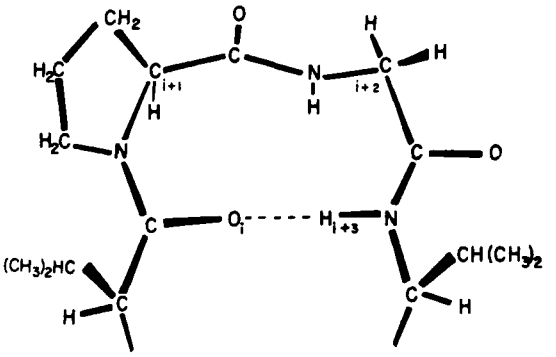

FIGURE 9. The β-turn formed by the pentapeptide, Val_1-Pro_2-Gly_3-Val_4-Gly_5. A similar β-turn with Pro as residue i + 1 and Gly as residue i + 3 is formed by the tetrapeptide Val-Pro-Gly-Gly. (From Urry, D. W., Cunningham, W. D., and Ohnishi, T., *Biochemistry*, 13, 609, 1974. With permission.)

pentapeptide (PPP) in Me_2SO-d_6 is given in Figure 12 with all resonances assigned. In the peptide NH region, the Val_1 NH and Val_4 NH resonances are well resolved but the Gly_3 NH and Gly_5 NH resonances are overlapping. Because the resonances are relatively broad for this high polymer, it is not possible to delineate the glycine resonances in Me_2SO-d_6 at any temperature. Any small differences in the Gly NH temperature dependences of chemical shift will be masked. Fortunately in the solvents of methanol and water the glycine NH resonances are satisfactorily resolved.

Temperature studies on the peptide NH chemical shifts are plotted in Figure 13 for three solvents. In Me_2SO-d_6, the Val_4 NH is seen at highest field with the least slope; the overlapping Gly_3 NH and Gly_5 NH resonances are at lowest field with a relatively low slope, and the Val_1 NH is seen in-between with the highest slope. In MeOH, a similar pattern is observed with the added feature that the glycine NHs are resolved with the Gly_3 NH at slightly higher field with a slightly lower slope. On titrating from methanol into water the glycine NH resonances cross such that in Figure 13C the Gly_3 NH is at slightly lower field with retention of the slightly lower slope. A most interesting feature of the water data is the abrupt change of slopes near 50°C, similar to that of the polytetrapeptide data of Figure 2D. Data were not plotted for trifluoroethanol because the resonances were resolvable only in the 45 to 70°C temperature range.

The temperature dependences of chemical shift in all four solvents for the peptide NH protons are listed in Table 9 along with the 0°C intercepts taken from the equation for the best least squares fit of the temperature data. As with the pentapeptide above, the Val_4 NH exhibits the lowest temperature coefficient, $d\delta/dT$, in each of the solvents, Me_2SO-d_6, methanol and water in the high temperature range (50 to 100°C). This delineation of the Val_4 NH as solvent shielded is reinforced by the solvent shift data in Table 10 where the peptide NH exhibiting the smallest change in chemical shift is the Val_4 NH in each of the three solvent pairs tabulated. Also to a lesser extent, the glycine NH protons are seen as solvent shielded in the temperature studies with the resolved Gly_3 NH in Me_2SO-d_6, MeOH, and water (both high and low temperature ranges) having a slightly lower temperature coefficient.

In order to get a qualitative estimate of the extents of shielding of the various peptide NHs, the mole fractions of shielding, calculated on the basis of the temperature data, are listed in Table 11. The Val_4 NH is the most shielded in Me_2SO-d_6, MeOH, and H_2O (50 to 100°C), with the greatest extent of shielding in Me_2SO-d_6 with a calculated probability of shielding of nearly 90% ($\chi_s^T = 0.87$). Presumably this shielding is due to

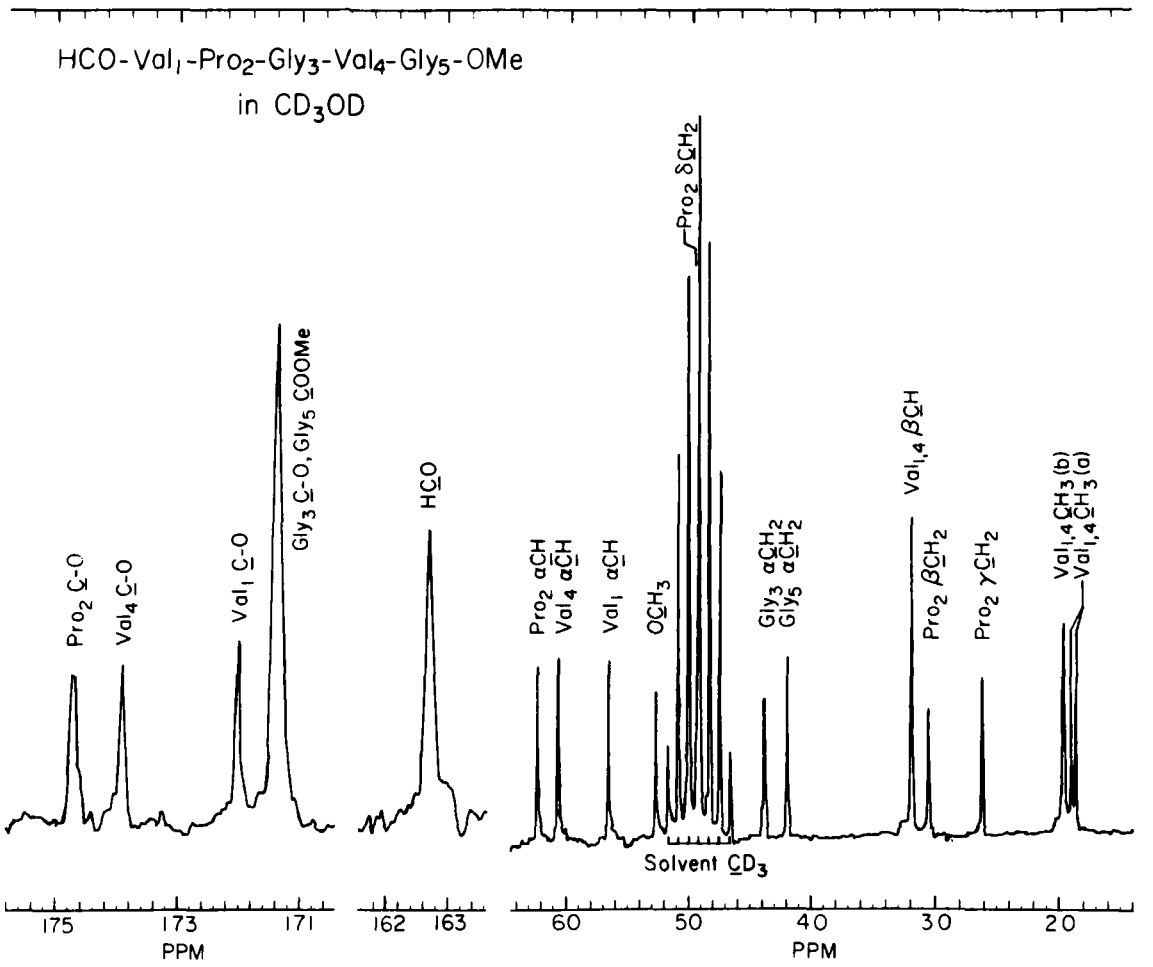

FIGURE 10. Carbon-13 magnetic resonance spectrum at 25.15 MHz of the pentapeptide, HCO-Val_1-Pro_2-Gly_3-Val_4-Gly_5-OMe, in CD_3OD at 33°C. All of the resonances are assigned. (From Urry, D. W., Mitchell, L. W., and Ohnishi, T., *Proc. Natl. Acad. Sci., USA*, 71(8), 3265, 1974. With permission.)

the Val_1 C-O as was demonstrated to be the case in the tetrapeptide series and suggested for the pentapeptide monomer. Polarized literal interpretations of the calculated value would be either that the hydrogen bond of Figure 9 occurs 90% of the time or that the hydrogen bond occurs all of the time but that it is at an angle that gives an effective 90% shielding. One should, however, be cautious about such literal interpretations. The reality may be a combination of the above tempered by an awareness of the complications inherent in the approach which were listed in some detail above. The major concerns in utilizing the data of Figure 13 and Tables 9, 10, and 11 are the source of shielding of the Gly_3 NH and Gly_5 NH protons in all the solvents and the unique introduction of substantial shielding of the Val_1 NH in H_2O at elevated temperatures. CMR data will be useful in this regard.

2. Carbon-13 Magnetic Resonance Studies

The CMR spectrum of the polypentapeptide in D_2O is given in Figure 14 with all resonances assigned. Table 12A contains the chemical shifts of the carbonyl carbon resonances of this polypentapeptide in Me_2SO-d_6, CD_3OD, CF_3CD_2OD, and D_2O at two temperatures, 20°C and 70°C. The latter represent the two temperature ranges exhibiting different slopes in the PMR studies included in Figure 13 and Table 9. Table 12B shows the calculated solvent shifts, reported both as the change in chemical shift with change in

TABLE 9

Temperature Dependence of Peptide NH Chemical Shifts of HCO-(Val_1-Pro_2-Gly_3-Val_4-Gly_5)$_{1\,8}$-Val-OMe in Several Solvents

PEPTIDE	Me_2SO-d_6		MeOH		CF_3CH_2OH[b]		H_2O(0-50°C)		H_2O(50-100°C)	
RESIDUE	$d\delta/dT_1$[a]	0°/Intercept	$d\delta/dT_2$[a]	0°/Intercept	$d\delta/dT_3$[a]	0°/Intercept	$d\delta/dT_{4a}$[a]	0°/Intercept	$d\delta/dT_{4b}$[a]	0°/Intercept
Val_1 NH	-7.3	8.19	-9.2	8.44	-8.3	7.78	-9.2	8.23	-6.0	8.07
Gly_3 NH	-5.2	8.38	-6.3	8.52	-5.9	7.91	-7.5	8.68	-6.1	8.62
Val_4 NH	-4.0	7.77	-4.9	8.07	-6.8	7.81	-7.8	8.15	-5.5	8.04
Gly_5 NH	-5.2	8.38	-7.3	8.67	-5.9	7.90	-8.2	8.64	-6.5	8.56

[a]Multiply by 10^{-3} to obtain coefficients in ppm/deg; multiply by 2.2 for Hz/10°C at 220 MHz.
[b]Temperature range 45 to 70°C. The resonances become broadened and not resolvable below 40°C.

TABLE 10

Solvent Dependence of HCO-(Val_1-Pro_2-Gly_3-Val_4-Gly_5)$_{1,8}$-Val-OMe Peptide NH Chemical Shifts at 20°C

PEPTIDE RESIDUE	1 Me_2SO-d_6	2 MeOH	3 [a] CF_3CH_2OH	4a H_2O	4b [b] H_2O	$\Delta\delta/\Delta S_{1,3}$	$\Delta\delta/\Delta S_{2,3}$	$\Delta\delta/\Delta S_{3,4}$
Val_1 NH	8.04	8.26	7.61	8.05	7.95	-0.43	-0.65	0.44
Gly_3 NH	8.28	8.43	7.79	8.53	8.50	-0.49	-0.64	0.74
Val_4 NH	7.69	7.98	7.67	7.99	7.93	-0.02	-0.31	0.32
Gly_5 NH	8.28	8.55	7.78	8.48	8.43	-0.50	-0.77	0.70

[a]20°C values are extrapolated from 45 to 70°C temperature data.
[b]Extrapolated high temperature data.

TABLE 11

Calculated Mole Fractions of Shielding for HCO-(Val_1-Pro_2-Gly_3-Val_4-Gly_5)$_{1,8}$-Val-OMe Based on Temperature Studies

PEPTIDE RESIDUE	Me_2SO-d_6	MeOH [a]	CF_3CH_2OH (45-70°C)	H_2O (0-50°C)	H_2O (50-100°C)
x_S^T (Val_1 NH)	0.15	0	(0)	0	0.62
x_S^T (Gly_3 NH)	0.61	0.50	(0.52)	0.33	0.63
x_S^T (Val_4 NH)	0.87	0.74	(0.30)	0.27	0.71
x_S^T (Gly_5 NH)	0.61	0.33	(0.52)	0.19	0.52

[a]For the methanol study the largest negative temperature coefficient was -9.2×10^{-3}. This was the value used for a_e^T.

solvent, $\Delta\delta/\Delta S_{i,j}$, and as the change in chemical shift calculated with respect to the carbonyl carbon resonance which was identified in the $\Delta\delta/\Delta S_{i,j}$ column as having shifted downfield the least.

A solvent titration at 40°C for the solvent pair 1 → 4, i.e., from Me_2SO-d_6 into D_2O, is plotted in Figure 15. The chemical shifts are plotted with respect to the Val_1 C-O which shifts downfield the least. The Val_1 C-O, as was expected (see Figure 9), is the most shielded and is then paired with the Val_4 NH. The substantial delineation of the Gly_5 C-O makes it a candidate for hydrogen bonding to one of the glycine NHs. In Me_2SO-d_6 both Gly NHs are equally shielded (see Table 11). This may be partially due to the overlapping of these resonances such that differences can not be detected. In H_2O (0 to 50°C), as seen in Tables 9 and 11, it is the Gly_3 NH that is preferentially shielded. This suggests a possible pairing of the Gly_5 C-O with the Gly_3 NH. The two smallest hydrogen bonded rings for this pairing are a 10-atom hydrogen bonded ring between the $Gly_{5,i-1}$ C-O and the $Gly_{3,i}$ NH and an 11-atom hydrogen bonded ring between $Gly_{5,i}$ C-O and $Gly_{3,i}$ NH. The ten-atom hydrogen bonded ring as noted in the polytetrapeptide study places L-Val and L-Pro at the corners of a β-turn, a seemingly strained structure. The 11-atom hydrogen bonded ring is indicated in Figure 16 with apparent favorable stereochemistry. This is also suggested on the basis of studies on the hexapeptide APGVGV (see below).

The secondary structure in Figure 16 introduces another possible hydrogen bond between the Gly_3 C-O and the Gly_5 NH. This seven-atom

hydrogen bonded ring occurs with an acute C-O···H-N hydrogen bond angle which could be expected to substantially shield the peptide NH without causing an equivalent shielding of the carbonyl. This would conform to the modest shielding of the Gly_3 C-O seen in the 1 → 4a and 1 → 4b solvent shifts listed in Table 12B. Using the values for the 1 → 4a, i,e., $Me_2SO\text{-}d_6$ → D_2O (20°C), solvent shift, it is instructive to calculate approximate mole fractions of shielding of the carbonyls, and to compare these values with the values in Table 11 on the peptide NHs. As with the polytetrapeptide data we take -1.02 for the denominator of Equation 3. For this titration then $a_s = -0.18$ and $a_e = 0.84$. The numerators are 0 - 0.84 for the Val_1 C-O, 0.81 - 0.84 for the Pro_2 C-O, 0.68 - 0.84 for the Gly_3 C-O, 0.84 - 0.84 for the Val_4 C-O, and 0.22 - 0.84 for the Gly_5 C-O, giving:

$$x_s^{st}(Val_1\ C\text{-}O) = 0.82 \quad x_s^{st}(Pro_2\ C\text{-}O) = 0.03$$

$$x_s^{st}(Gly_3\ C\text{-}O) = 0.16 \quad x_s^{st}(Val_4\ C\text{-}O) = 0$$

$$x_s^{st}(Gly_5\ C\text{-}O) = 0.61.$$

Since the titration tends to reflect the situation in $Me_2SO\text{-}d_6$ as discussed for the polytetrapeptide, these values may be compared to those in that solvent in Table 11. The Val_1 C-O pairs with the Val_4 NH, the Gly_5 C-O can be paired with the Gly_3 NH as discussed above, and the Gly_3 C-O can be paired with the Gly_5 NH with the carbonyl being less shielded due to the acute hydrogen bond angle of the seven-atom hydrogen bonded ring (see Figure 16).

It is tempting to carry the analysis further to a possible conformation in D_2O at elevated temperatures because of seemingly correlated increases in shielding of a peptide NH and a peptide C-O. On raising the temperature in H_2O, a dramatic increase in shielding of the Val_1 NH from 0 at low temperatures to 0.62 at elevated temperatures is observed (Note Figure 13, Table 9, and the calculated values for mole fraction of shielding in Table 11). Looking at the CMR data in Table 12B, the only significant change in carbonyl shielding on raising the temperature occurs with the Val_4 C-O. This suggests the introduction of hydrogen bonding between the Val_1 NH and the Val_4 C-O:

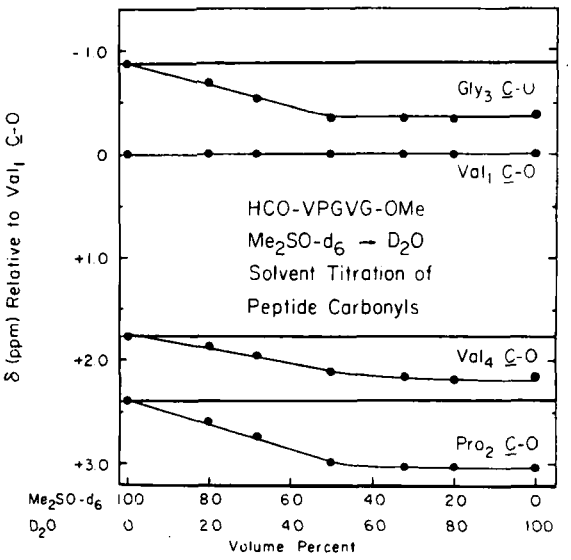

FIGURE 11. Solvent titration ($Me_2SO\text{-}d_6\text{-}D_2O$) of the HCO-VPGVG-OMe peptide carbonyl carbon resonances. The Val_1 C-O is taken as the reference. The other peptide carbonyl carbon resonances are seen to shift systematically downfield as the volume percent of D_2O is increased to about 50%. This result is interpreted to indicate that the Val_1 C-O is shielded from the solvent. (From Urry, D. W., Mitchell, L. W., and Ohnishi, T., *Proc. Natl. Acad. Sci. USA*, 71(8), 3265, 1974. With permission.)

Interestingly, this can be readily achieved with the structure in Figure 16 by small rotations of the $Val_{4,i} - Gly_{5,i}$ peptide moiety and the $Gly_{5,i-1} - Val_{1,i}$ peptide moiety. This results in a decrease in hydrogen bond shielding of the Gly_5 NH which becomes partially replaced by steric effects of the resulting loose β-spiral shown in Figure 17.

A β-spiral is defined as a repeat along an axis of a conformational unit in which the β-turn is a prominent feature. The structure shown in Figure 17 has the above defined conformational features repeating along the spiral axis with approximately 2.8 pentapeptide repeats per turn of spiral and about a 3.2 Å translation per repeat along the spiral axis. Topologically it is made up of alternating hydrophobic and hydrophilic ridges running lengthwise of the structure in the form of a long spiral with one complete turn of the spiralling ridges every 100 to 120 Å. Whether or not this working model is the best description of the dynamic polypentapeptide in its most ordered state, it does characterize the class of structures that one can expect the polypentapeptide to assume, and it is easy to see how such structures

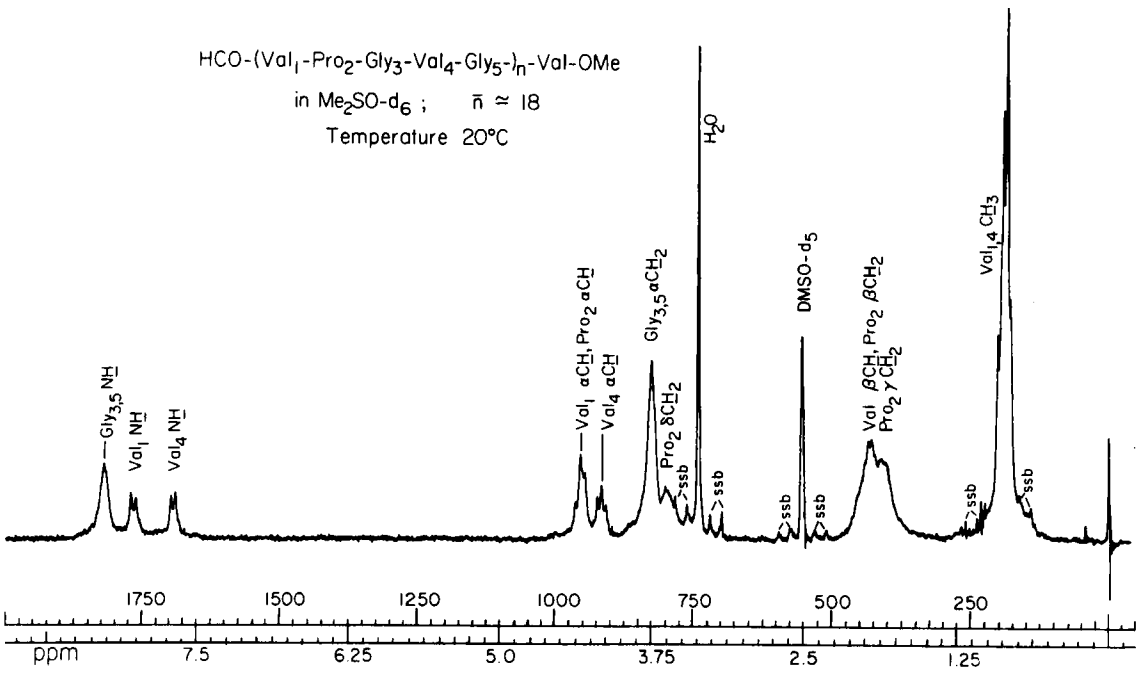

FIGURE 12. Proton magnetic resonance spectrum at 220 MHz in Me_2SO at 20°C of the polypentapeptide of elastin, HCO-(Val_1-Pro_2-Gly_3-Val_4-Gly_5)$_n$-Val-OMe, where n ≅ 18. All resonances are assigned; ssb, spinning side bands. (From Urry, D. W., Mitchell, L. W., Ohnishi, T., and Long, M. M., *J. Mol. Biol.*, 96, 101, 1975. With permission.)

could associate by hydrophobic interactions with an intertwining of chains to form a fibrillar unit.

V. THE REPEAT HEXAPEPTIDE OF ELASTIN

In the hexapeptide series the monomer (APGVGV) as well as the five additional cyclically varied permutations, the decapeptide and pentadecapeptide oligomers, i.e., $(APGVGV)_n$ where n = 2 and 3, and high polymers with the average values of n being about 20 or more have been synthesized. As with the previous peptides, these have been studied by spectroscopic methods with a primary objective being the evaluation of solution secondary structure. In the following, proton and carbon-13 magnetic resonance data will be presented and discussed for the monomer, APGVGV, a permutation of the monomer, PGVGVA, and for the polyhexapeptide.

A. The Monomers, HCO-Ala_1-Pro_2-Gly_3-Val_4-Gly_5-Val_6-OMe and Boc-Pro_2-Gly_3-Val_4-Gly_5-Val_6-Ala_1-OMe[39,46]

In the hexamer, $A_1P_2G_3V_4G_5V_6$, decoupling provides the assignment of the Ala_1 NH, multiplet structure separates the glycine and valine NH resonances, and chemical modification of the carboxyl terminus allows assignment of the Val_4 NH and the Val_6 NH resonances. This leaves the glycine resonances to be delineated. Synthesis of HCO-$A_1P_2G_3(d_2)V_4G_5V_6$-OMe results in a singlet for the $Gly_3(d_2)$NH resonance as seen in Figure 18. In the above manner the assignment of the NH resonances were achieved. The temperature dependences of the peptide NH protons in the four solvents, Me_2SO-d_6, MeOH, CF_3CH_2OH, and H_2O, are reported in Table 13.

In what is now a well-established pattern, the Val_4 NH exhibits the least slope with the exception of Me_2SO-d_6, where the Gly_3 NH has a slightly lower slope. A decreased slope in the Gly_3 NH was also observed above in the pentamer series (see Figure 13 and Tables 7 and 9), but the hexamer is the first time the Gly_3 NH temperature coefficient was of a lesser magnitude than the Val_4 NH. Since this occurs in Me_2SO, it provides an opportunity to define the source of shielding by employing the CMR methods. First, however, we should note the peptide NH solvent shift data in

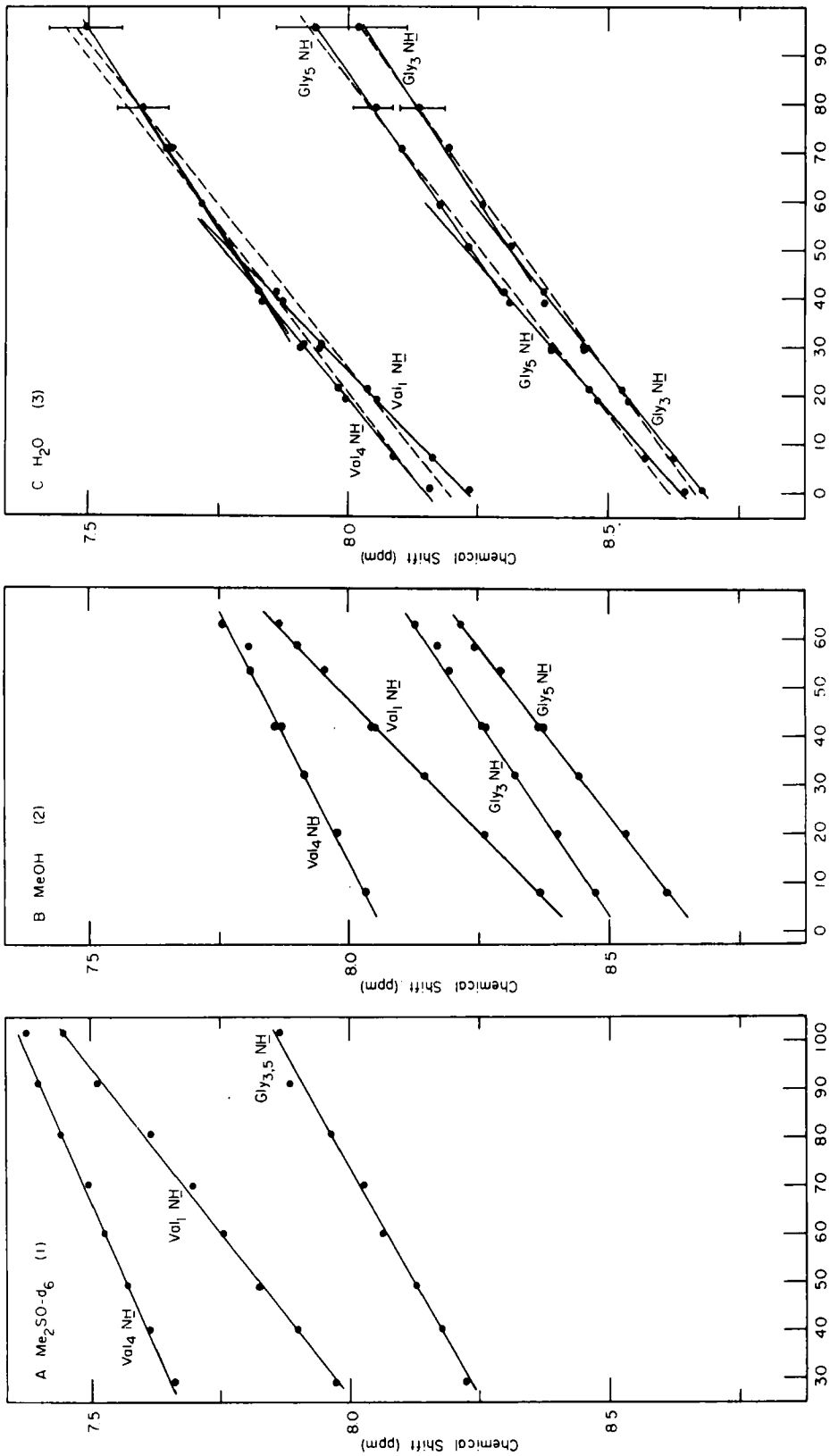

FIGURE 13. Temperature dependence of the proton chemical shift of HCO-(Val-Pro-Gly-Val-Gly)$_n$-Val-OMe in dimethyl sulfoxide, methanol, and water.

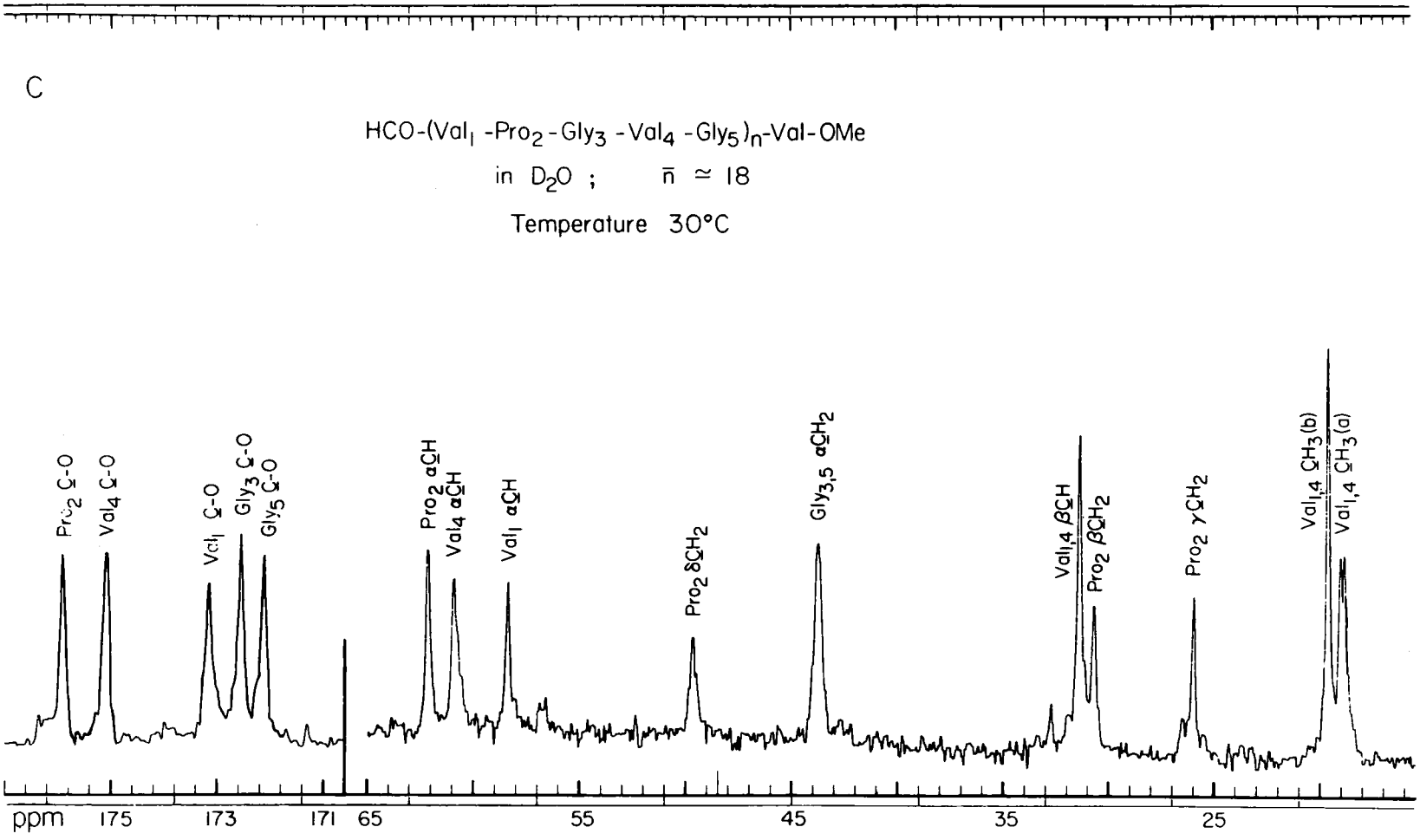

FIGURE 14. ^{13}C Magnetic resonance spectrum at 25 MHz and 30°C of the elastin polypentapeptide, HCO-(Val$_1$-Pro$_2$-Gly$_3$-Val$_4$-Gly$_5$)$_n$-Val-OMe, where n ≅ 18. All resonances are assigned. In D_2O. (From Urry, D. W., Mitchell, L. W., Ohnishi, T., and Long, M. M., *J. Mol. Biol.*, 96, 101, 1975. With permission.)

TABLE 12

Solvent Dependence of HCO-(Val$_1$-Pro$_2$-Gly$_3$-Val$_4$-Gly$_5$)$_{1\,8}$-Val-OMe Peptide Carbonyl Chemical Shifts

A. Chemical shifts

PEPTIDE RESIDUE	1 Me_2SO-d_6	2 CD_3OD	3 CF_3CD_2OD	4a D_2O (20°C)	4b D_2O (70°C)
Val_1 C-O	169.79	172.41	173.57	172.61	172.54
Pro_2 C-O	171.73	174.73	175.90	175.36	175.34
Gly_3 C-O	168.52	171.34	172.70	172.02	172.04
Val_4 C-O	170.90	173.76	175.07	174.56	174.32
Gly_5 C-O	168.52	171.19	171.97	171.56	171.59

B. Solvent Shifts

PEPTIDE RESIDUE	1 → 2		1 → 3		1 → 4a		1 → 4b		4a → 4b
	$\Delta\delta/\Delta S_{1,2}$	$\Delta\delta_{m1}$[a]	$\Delta\delta/\Delta S_{1,3}$	$\Delta\delta_{m5}$[a]	$\Delta\delta/\Delta S_{1,4a}$	$\Delta\delta_{m1}$[a]	$\Delta\delta/\Delta S_{1,4b}$	$\Delta\delta_{m1}$[a]	$\Delta\delta/\Delta S_{4a,4b}$
Val_1 C-O	2.62	0	3.78	0.33	2.82	0	2.75	0	-0.07
Pro_2 C-O	3.00	0.38	4.17	0.72	3.63	0.81	3.61	0.86	-0.02
Gly_3 C-O	2.82	0.20	4.18	0.73	3.50	0.68	3.52	0.77	0.02
Val_4 C-O	2.80	0.24	4.17	0.72	3.66	0.84	3.42	0.67	-0.24
Gly_5 C-O	2.67	0.05	3.45	0	3.04	0.22	3.07	0.32	0.03

[a] $\Delta\delta_{mi}$ defined in Table 6.

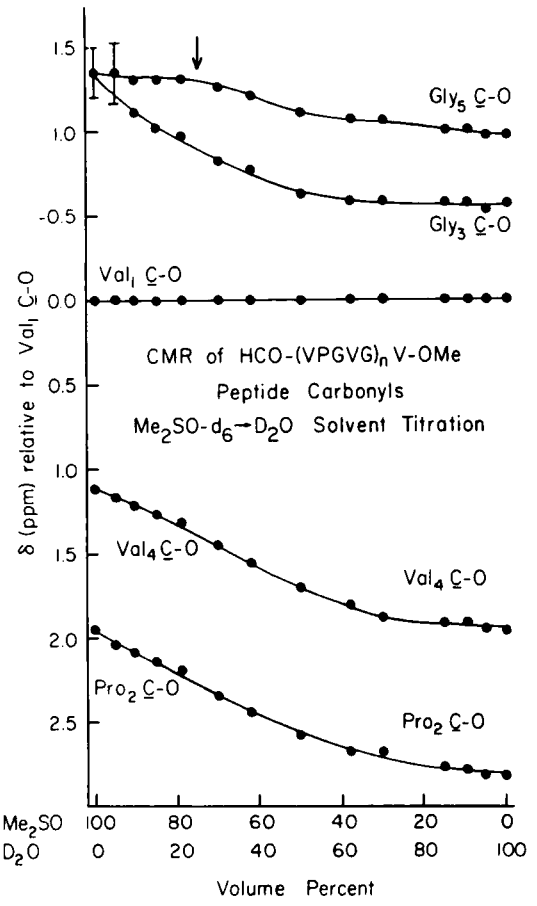

FIGURE 15. Solvent titration, $Me_2SO \rightarrow D_2O$ taken at 40°C of the peptide carbonyl carbon resonances of the elastin polypentapeptide, HCO-(Val_1-Pro_2-Gly_3-Val_4-Gly_5)$_n$-Val-OMe, where n ≅ 18. At this temperature, coacervation occurs in D_2O and is present up to 80% Me_2SO. The spectra of the coacervate are as readily obtained as when the molecules are molecularly dispersed, making this an $Me_2SO \rightarrow$ coacervate titration. (From Urry, D. W., Mitchell, L. W., Ohnishi, T., and Long, M. M., *J. Mol. Biol.*, 96, 101, 1975. With permission.)

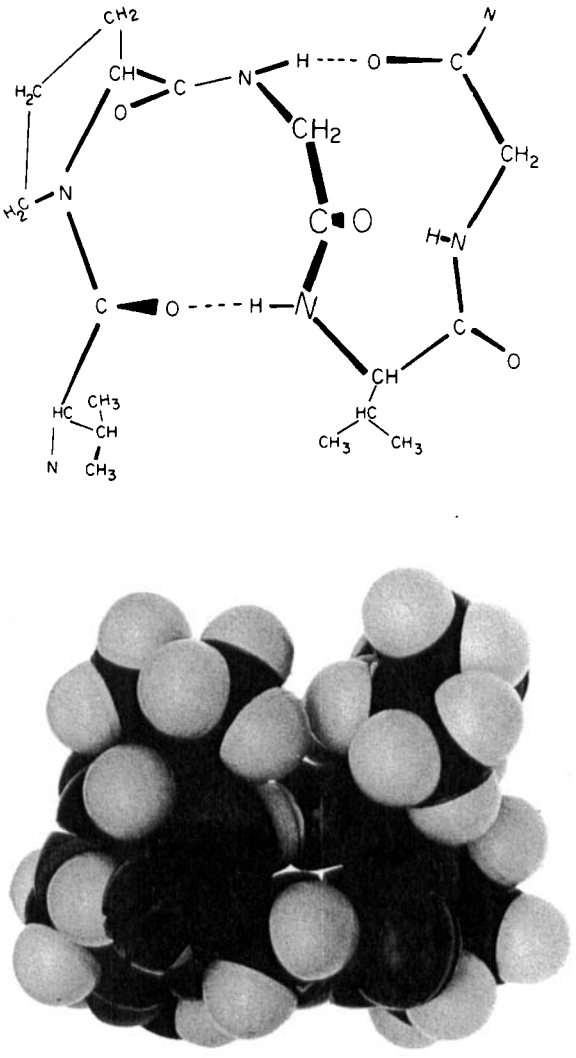

FIGURE 16. Proposed secondary structural features of the repeating pentapeptide unit in the polypentapeptide of elastin. See text for discussion. (From Urry, D. W., Mitchell, L. W., Ohnishi, T., and Long, M. M., *J. Mol. Biol.*, 96, 101, 1975. With permission.)

Table 14 which continue to delineate the Val_4 NH most significantly.

The CMR spectrum of all of the resonances of HCO-$A_1P_2G_3(d_2)V_4G_5V_6$-OMe are contained in Figure 19. The resonance assignments are also included. In passing it may be noted that the Gly_3 (d_2) C-O resonance is less intense than the other resonances. This is because there is no nuclear Overhauser enhancement (X 2+) for the deuterated residue which derives from proton broad band decoupling. The differences in intensity facilitate following the resonances during solvent titrations where the glycine carbonyl carbon resonances cross. Chemical shifts of the carbonyl carbon resonances are listed in Table 15A, for the four solvents of interest. The solvent shifts, $\Delta\delta/\Delta S_{i,j}$, are tabulated in Table 15B along with the solvent shifts calculated relative to the carbonyl carbon, δ_{mi}, which moves downfield least on going from Me_2SO-d_6 into the second solvent. For the first time in these series of elastin peptides a residue other than the $residue_1$ C-O, the Gly_5 C-O, shows the least solvent shift. A representative solvent titration is seen in Figure 20, where it was helpful to have the $Gly_3(d_2)$ C-O resonance distinguished by its lower intensity to

TABLE 13

Temperature Dependence of HCO-Ala$_1$-Pro$_2$-Gly$_3$-Val$_4$-Gly$_5$-Val$_6$-OMe Peptide NH Chemical Shifts

PEPTIDE	Me_2SO-d_6		MeOH		CF_3CH_2OH		H_2O	
RESIDUE	$d\delta/dT_1$[a]	0°/Intercept	$d\delta/dT_2$[a]	0°/Intercept	$d\delta/dT_3$[a]	0°/Intercept	$d\delta/dT_4$[a]	0°/Intercept
Ala_1 NH	-5.9	8.45	-7.5	8.64	-8.3	7.85	-7.7	8.54
Gly_3 NH	-4.0	8.28	-6.7	8.56	-7.6	7.94	-7.0	8.68
Val_4 NH	-4.3	7.78	-3.7	8.01	-5.0	7.74	-6.4	8.11
Gly_5 NH	-5.0	8.36	-7.6	8.79	-6.6	8.01	-7.4	8.65
Val_6 NH	-5.6	8.18	-7.4	8.29	-5.1	7.33	-8.3	8.31

[a]Multiply by 10^{-3} to obtain temperature coefficients in ppm/deg.

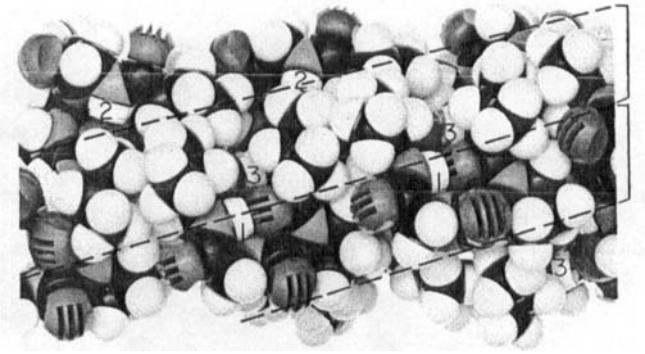

1- Val_4 NH···O-C Val_1
2- Gly_3 NH···O-C Gly_5
3- Val_1 NH···O-C Val_4

FIGURE 17. Space-filling model of the polypentapeptide, HCO-(Val$_1$-Pro$_2$-Gly$_3$-Val$_4$-Gly$_5$)$_n$-Val-OMe, β-spiral.

TABLE 14

Solvent Dependence of HCO-Ala$_1$-Pro$_2$-Gly$_3$-Val$_4$-Gly$_5$-Val$_6$-OMe Peptide NH Chemical Shifts at 20°C

PEPTIDE RESIDUE	1 Me_2SO-d_6	2 MeOH	3 CF_3CH_2OH	4 H_2O	$\Delta\delta/\Delta S_{1,3}$	$\Delta\delta/\Delta S_{2,3}$	$\Delta\delta/\Delta S_{3,4}$
Ala_1 NH	8.33	8.49	7.68	8.39	-0.65	-0.81	0.71
Gly_3 NH	8.20	8.43	7.79	8.54	-0.41	-0.64	0.75
Val_4 NH	7.69	7.94	7.64	7.98	-0.05	-0.30	0.34
Gly_5 NH	8.26	8.65	7.88	8.50	-0.38	-0.77	0.62
Val_6 NH	8.17	8.14	7.23	8.14	-0.94	-0.91	0.91

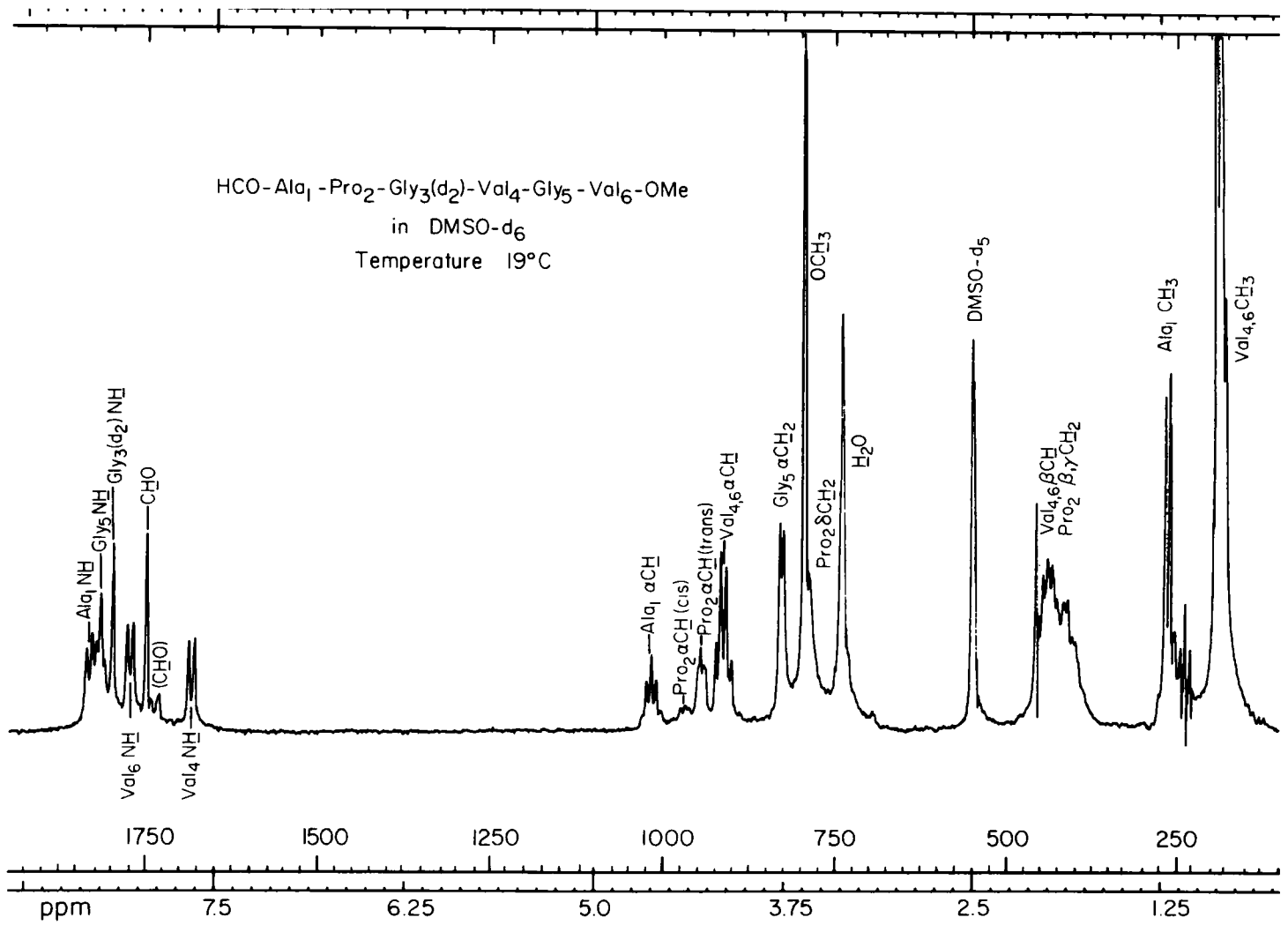

FIGURE 18. Proton magnetic resonance spectrum of HCO-Ala_1-Pro_2-$Gly_3(d_2)$-Val_4-Gly_5-Val_6-OMe at 220 MHz in Me_2SO-d_6 and at 19°C. The assignment of all resonances are indicated. This work provides unambiguous assignment of the glycine resonances which is necessary before the secondary structure of the hexapeptide of elastin can be deduced. -$Gly_3(d_2)$- [$^2H_2$]Gly_3-; -DMSO-d_6, Me_2SO-d_6. (From Urry, D. W., Mitchell, L. W., and Ohnishi, T., *Biochim. Biophys. Acta*, 393, 296, 1975. With permission.)

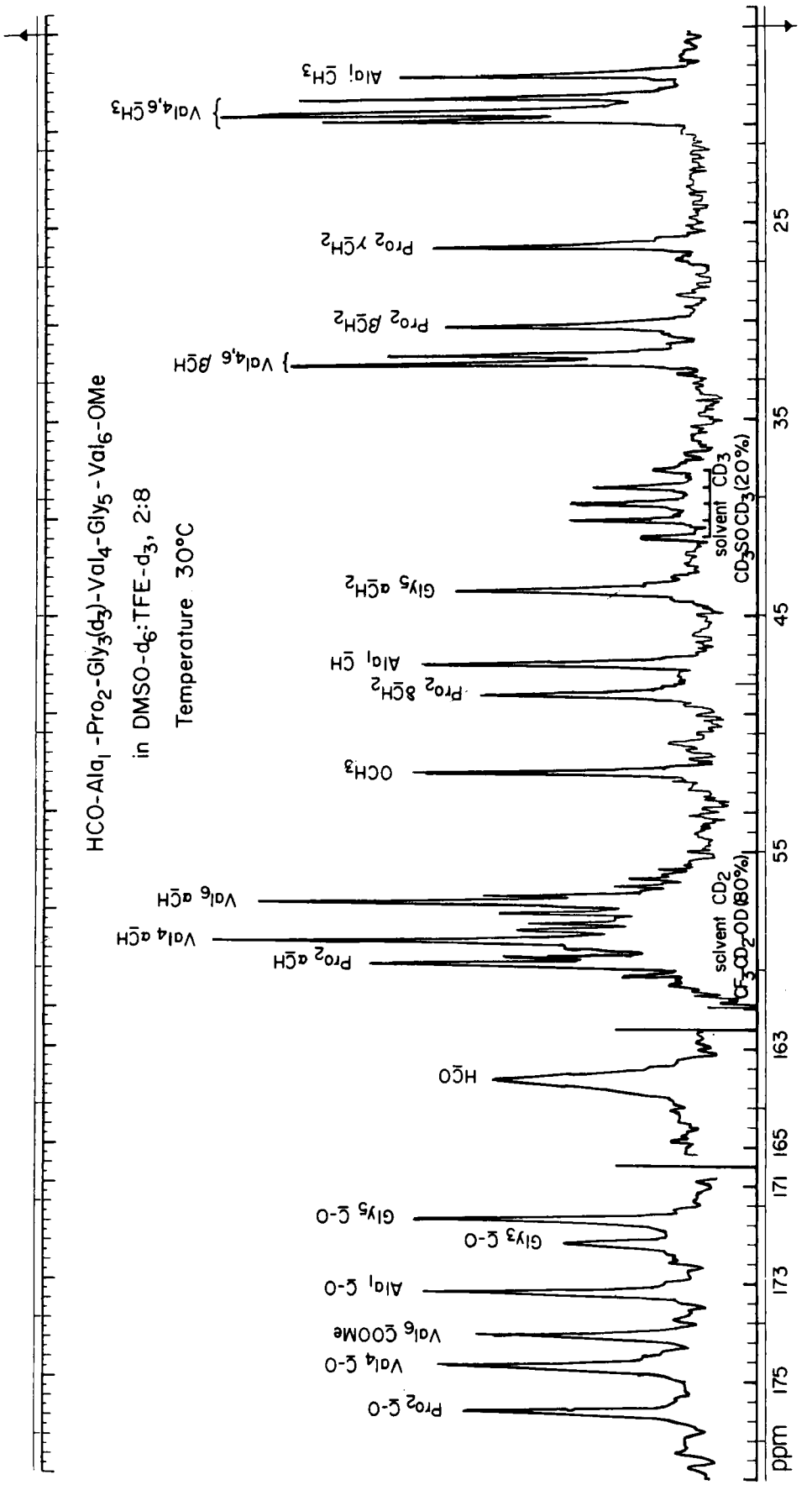

FIGURE 19. Carbon-13 magnetic resonance spectrum of HCO-Ala_1-Pro_2-$Gly_3(d_2)$ Val_4-Gly_5-Val_6-OMe at 25 MHz in Me_2SO-d_6/trifluoroethanol-d_3 2:8 and at 30°C. Chemical shifts are given with respect to an internal reference of $(CH_3)_4Si$. The assignments of all the resonances are given. Note that the $Gly_3(d_2)$ C-O resonance near 172 ppm is less intense than the other carbonyl resonances. This allows the $Gly_3(d_2)$ C-O resonance to be distinguished from the Gly_5 C-O during the solvent titrations. -$Gly_3(d_2)$-; -$[^2H_2]Gly_3$-; DMSO-d_6/TFE-d_3, Me_2SO-d_6/trifluoroethanol-d_3. (From Urry, D. W., Mitchell, L. W., and Ohnishi, T., *Biochim. Biophys. Acta*, 393, 296, 1975. With permission.)

TABLE 15

Solvent Dependence of HCO-Ala_1-Pro_2-Gly_3-Val_4-Gly_5-Val_6-OMe Peptide Carbonyl Carbon Chemical Shift at 23°C

A. Chemical shifts

PEPTIDE RESIDUE	1 Me_2SO-d_6	2 CD_3OD	3 CF_3CD_2OD	4 D_2O
Ala_1 C-O	170.22	172.65	173.67	173.71
Pro_2 C-O	171.77	174.93	176.09	176.00
Gly_3 C-O	168.62	171.39	172.79	172.46
Val_4 C-O	171.00	173.86	175.37	175.03
Gly_5 C-O	168.81	171.19	172.12	172.31

B. Solvent shifts

PEPTIDE RESIDUE	1 → 2		1 → 3		1 → 4	
	$\Delta\delta/\Delta S_{1,2}$	$\Delta\delta_{m5}$	$\Delta\delta/\Delta S_{1,3}$	$\Delta\delta_{m5}$	$\Delta\delta/\Delta S_{1,4}$	$\Delta\delta_{m1}$
Ala_1 C-O	2.43	0.05	3.45	0.14	3.49	0
Pro_2 C-O	3.16	0.78	4.32	1.01	4.23	0.74
Gly_3 C-O	2.77	0.39	4.17	0.86	3.84	0.34
Val_4 C-O	2.86	0.48	4.37	1.06	4.03	0.53
Gly_5 C-O	2.38	0	3.31	0	3.50	0.01

be certain that it was the Gly_5 C-O which showed the low solvent shift rather than the Gly_3 C-O.

This firm identification of the Gly_5 C-O as exhibiting shielding equivalent to or possibly slightly greater than that of the Ala_1 C-O, i.e., the carbonyl preceding proline, provides the basis for describing the source of shielding of the Val_4 NH and Gly_3 NH observed in the temperature studies (see Table 13).

Calculated mole fractions of shielding for both the peptide NHs based on the PMR temperature studies and the peptide C-Os based on the CMR solvent shift studies are contained in Table 16. In the Me_2SO-d_6 column in Part A, the most shielded peptide NHs are the Gly_3 NH and the Val_4 NH with about 90% and 80% shielding, respectively. Recalling that the CMR solvent shift studies provide more information on the situation in the first solvent Me_2SO-d_6 than on the second solvent, we look to Part B of Table 16 for appropriate pairings which could explain the shielding in terms of intramolecular hydrogen bonds. It is reasonable to continue to take the same β-turn for the hexapeptide, for which the evidence was so apparent for the tetrapeptide and pentapeptide, that is, the Residue$_1$ C-O · · · HN Residue$_4$ hydrogen bond which places Pro_2 and Gly_3 at the corners of a β-turn. This assumption is demonstrated to be correct in an interesting study below on the $P_2G_3V_4G_5V_6A_1$ permutation of the hexapeptide monomer. Having paired the Val_4 NH with the Ala_1 C-O leaves the Gly_5 C-O to pair with the Gly_3 NH which are the pairings that would follow from a strict comparison of the calculated mole fractions of shielding. Thus the two major secondary structural features for the hexamer are as proposed for the pentapeptide (see Figure 16).

Boc-Pro_2-Gly_3-Val_4-Gly_5-Val_6-Ala_1-OMe – At room temperature in the PMR this hexapeptide exhibits an interesting interconversion between

TABLE 16

Calculated Mole Fractions of Shielding of Peptide NH and Peptide Carbonyls of HCO-Ala$_1$-Pro$_2$-Gly$_3$-Val$_4$-Gly$_5$-Val$_6$-OMe

A.

PEPTIDE RESIDUE	1 Me_2SO-d_6	2 MeOH	3 CF_3CH_2OH	4 H_2O
x_S^T (Ala_1 NH)	0.46	0.04	0	0.32
x_S^T (Gly_3 NH)	0.87	0.22	0.16	0.47
x_S^T (Val_4 NH)	0.80	0.89	0.77	0.62
x_S^T (Gly_5 NH)	0.65	0.01	0.40	0.38
x_S^T (Val_6 NH)	0.52	0.04	0.74	0.11

B.

PEPTIDE RESIDUE	1 → 2	1 → 3	1 → 4
x_S^{st} (Ala_1 C-O)	0.94	0.84	0.73
x_S^{st} (Pro_2 C-O)	0	0.05	0
x_S^{st} (Gly_3 C-O)	0.50	0.18	0.39
x_S^{st} (Val_4 C-O)	0.38	0.04	0.21
x_S^{st} (Gly_5 C-O)	1.0	0.96	0.72

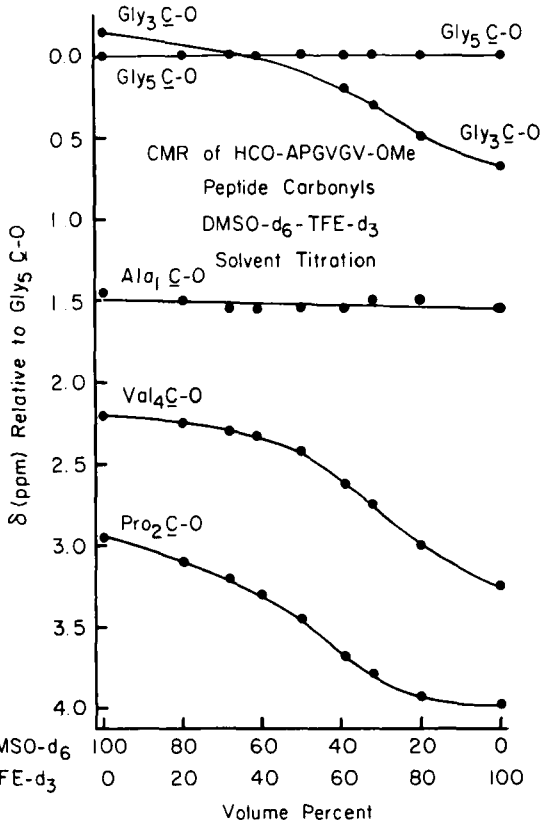

FIGURE 20. Solvent titration Me_2SO-d_6 → trifluoroethanol-d_3 of the peptide carbonyls of HCO-Ala$_1$-Pro$_2$-Gly$_3$(d_2)-Val$_4$-Gly$_5$-Val$_6$-OMe plotted with respect to the Gly$_5$ C-O resonance. Note that the Gly$_3$, Val$_4$, and Pro$_2$ C-O resonances show a greater solvent sensitivity shifting further downfield on addition of trifluoroethanol-d_3 which indicates a greater solvent exposure of these three carbonyls. DMSO-d_6/TFE-d_3, Me_2SO-d_6/trifluoroethanol; CMR, Carbon-13 magnetic resonance. (From Urry, D. W., Mitchell, L. W., and Ohnishi, T., *Biochim. Biophys. Acta*, 393, 296, 1975. With permission.)

two conformational states which is slow relative to the 220-MHz observation frequency. Two resonance lines are observed for the Gly$_3$ NH and Val$_4$ NH protons, whereas the other peptide NHs give single lines as shown in Figure 21. At high field near 1.3 ppm, the Boc CH_3 singlet resonance is also split into two resonances and at midfield the *cis* Pro αCH resonance, which is only a minor peak indicating about 10 to 15% occurrence in Figure 18, has become larger indicating about a 55% occurrence. This means that the two states are a *cis* and a *trans* Boc carbonyl-N Pro bond. Raising the temperature shows the Gly$_3$ NH and Val$_4$ NH resonances to be coalesced though broad at 49°C (see Figure 21). The resonances sharpen and regain appropriate line width at about 70°C. The formyl derivative shows the same two states of nearly equal population in Me_2SO-d_6, but it requires a higher temperature before coalescence occurs near 100°C. These data have been analyzed to obtain the enthalpies and entropies of activation for the *cis-trans* conversion.[39] For the Boc derivative $\Delta H^{\ddagger}$ = 15.5 kcal/mol and $\Delta S^{\ddagger}$ = 1.9 entropy units and for the HCO derivative $\Delta H^{\ddagger}$ = 18.5 kcal/mol and $\Delta S^{\ddagger}$ = 1.9 entropy units.

The particular interest this *cis-trans* isomerization has for PMR analysis of hexapeptide secondary structure is that the above described C-O$_1$ · · · H-N$_4$ β-turn requires a *trans* X-Pro peptide bond. The temperature data, plotted in Figure 22, show the effects of the *cis* and *trans* isomers on the chemical shifts and slopes of the peptide NH resonances. The results are explicable in terms of resonances A representing the *trans* isomer in the Pro$_{i+1}$-Gly$_{i+2}$ β-turn. The observa-

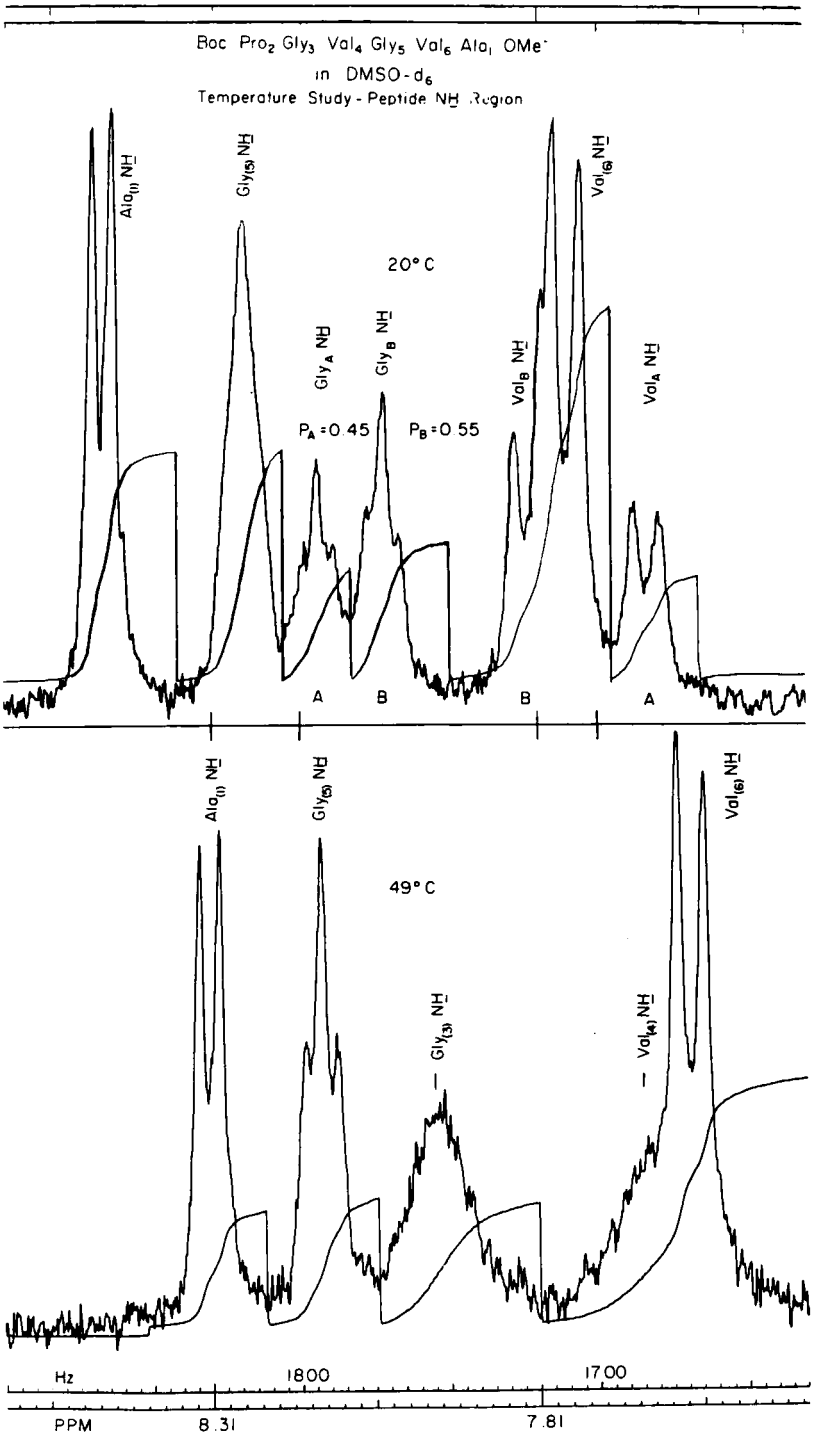

FIGURE 21. Peptide NH region of Boc-Pro_2-Gly_3-Val_4-Gly_5-Val_6-Ala_1-OMe in Me_2SO-d_6. In the upper figure, the Val_4 NH resonance at 20°C is split, giving two resolvable conformations. A glycine resonance also is split into Conformers A and B with probabilities P_A = 0.45 and P_B = 0.55. In the lower figure, the split resonances are seen to coalesce at 49°C. (From Urry, D. W. and Ohnishi, T., *Peptides, Polypeptides and Proteins*, Blout, E. R., Bovey, F. A., Goodman, M., and Lotan, N., Eds., John Wiley & Sons, New York, 1974, 230. With permission.)

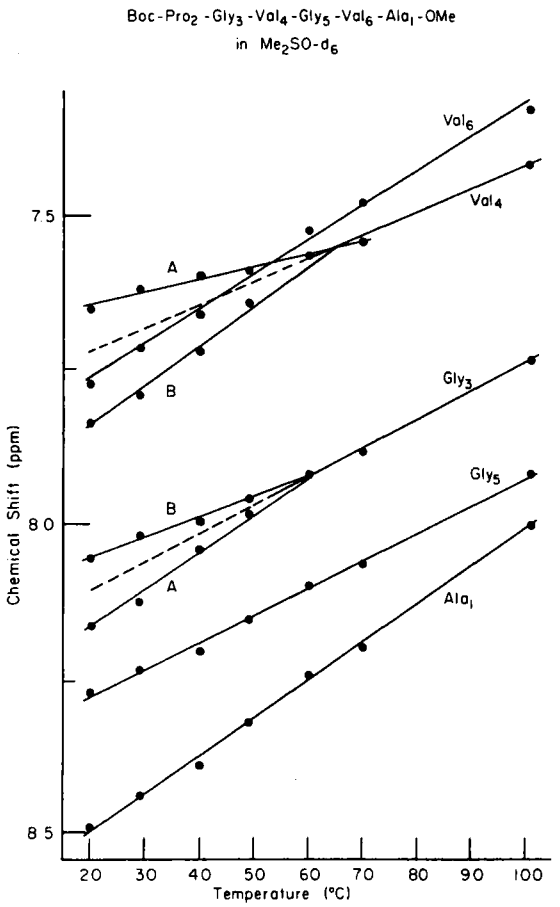

FIGURE 22. Temperature dependence of the proton chemical shift of Boc-Pro_2-Gly_3-Val_4-Gly_5-Val_6-Ala_1-OMe in dimethyl sulfoxide.

tion that the Val_4 NH is sensitive to the orientation of the $residue_1$ carbonyl and that its chemical shift splitting is greater than for the Gly_3 NH are indicative of a direct interaction. More specifically, however, the A resonance of Val_4 NH is at high field and the mean position of the A and B components as well as the slope after coalescence demonstrates a low temperature coefficient. These, of course, are the characteristics of $Residue_4$ NH in a β-turn and therefore argue for the $Residue_1$ C-O · · · HN Val_4 β-turn in the hexapeptide.

B. The Polyhexapeptide, HCO-Val-(Ala_1-Pro_2-Gly_3-Val_4-Gly_5-Val_6)$_{18}$-OMe[47]

The polyhexapeptide exhibits a solubility behavior which distinguishes it from the polytetrapeptide and the polypentapeptide; it has a limited solubility in methanol. Preparations could be purified by washing the high polymer in methanol. The methanol washed (but Me_2SO-d_6, trifluoroethanol and water soluble) material gave the cleanest PMR and CMR spectra. This solubility property is similar to that of α-elastin, a 70,000-dalton oxalic acid fragmentation product of fibrous elastin.[53,54] α-Elastin has limited solubility in methanol but is soluble in the other solvents. Because of this there will be no nuclear magnetic resonance data reported for the polyhexapeptide in CH_3OH and CD_3OD solvents.

1. Proton Magnetic Resonance Studies

The complete proton magnetic resonance spectrum of HCO-Val-(Ala_1-Pro_2-Gly_3-Val_4-Gly_5-Val_6)$_n$-OMe, where the average value for n is approximately 18, is seen in Figure 23. Partial assignments of the peptide NH resonances were achieved by decoupling experiments at elevated temperatures which define the Ala_1 NH resonance, and clearly delineate the two Val NH resonances from the two Gly NH resonances. The breadth and overlap of the resonances in the high polymer tend to make assignment based on multiplet structure not as definitive as in the monomers and oligomers. Where separation of the two glycine and two valine resonances occurred, the monomer and oligomer data were used independently to make the assignments in each solvent, and the self-consistency of these assignments was verified from solvent to solvent by solvent titrations.

The temperature studies of the peptide NH chemical shifts in the three solvents, Me_2SO-d_6, CF_3CH_2OH, and H_2O, are plotted in Figure 24. In each case it is the Ala_1 NH which shows the highest slope, and presumably the greatest exposure to solvent. The Val_4 NH shows the lowest slope except in CF_3CH_2OH where the Val_6 NH exhibits a somewhat lower slope. The Val_4 NH is consistently highly shielded from the solvent. As with the polytetrapeptide and the polypentapeptide, an abrupt change in slope is observed in water near 60°C, indicating a conformational change with greater shielding of the peptide NHs from the solvent in the higher temperature range. A change to increased order in a peptide on increasing temperature is indicative of destructuring of the water molecules surrounding exposed

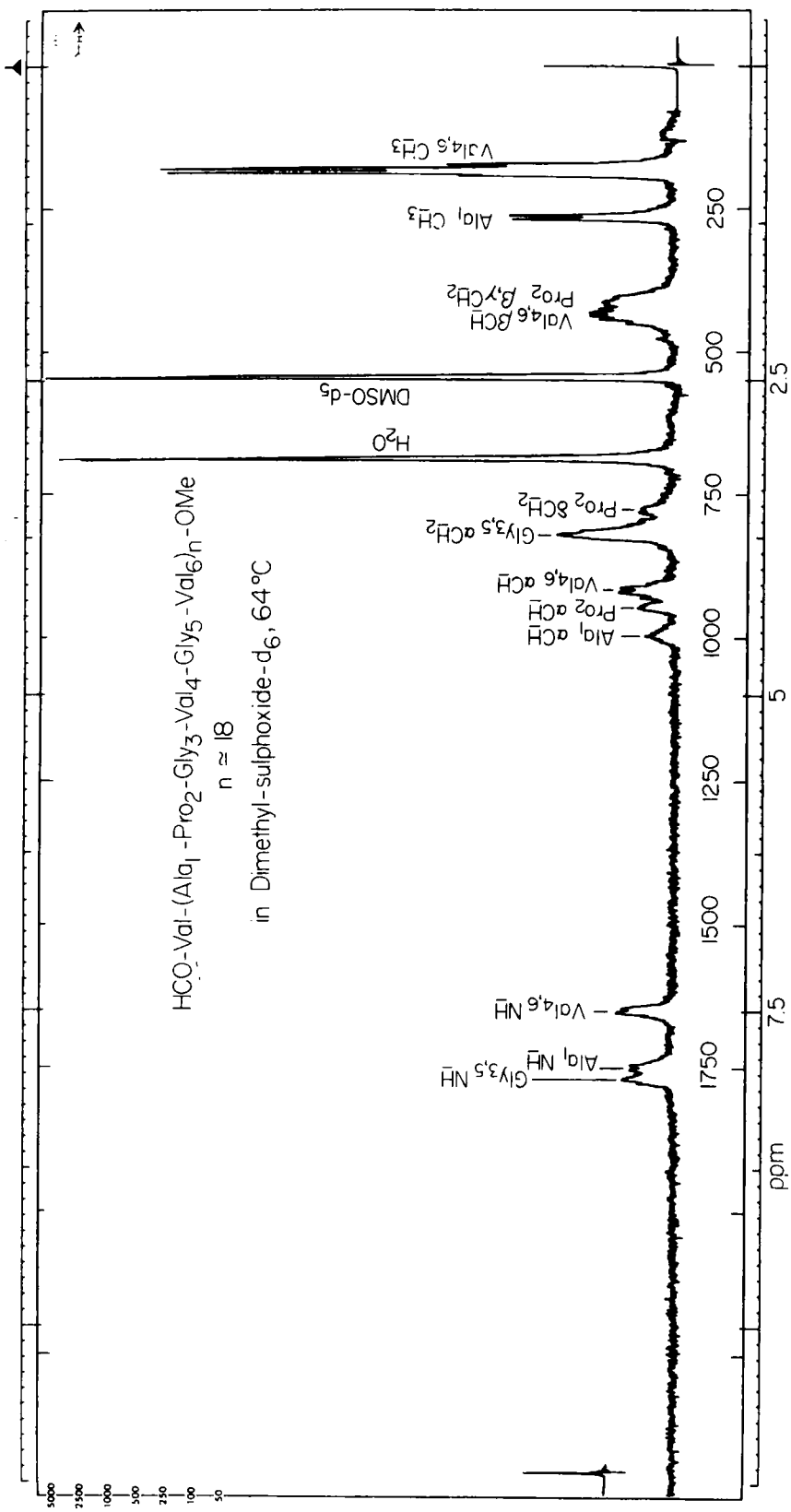

FIGURE 23. Proton magnetic resonance spectrum at 220 MHz of HCO-Val-(Ala_1-Pro_2-Gly_3-Val_4-Gly_5-Val_6)$_{1\,8}$-OMe in Me_2SO-d_6 at 64°C. Chemical shifts are given with respect to an internal reference of tetramethyl silane (TMS). (From Urry, D. W., Ohnishi, T., Long, M. M., and Mitchell, L. W., *Int. J. Pept. Protein Res.*, 7, 367, 1975. With permission.)

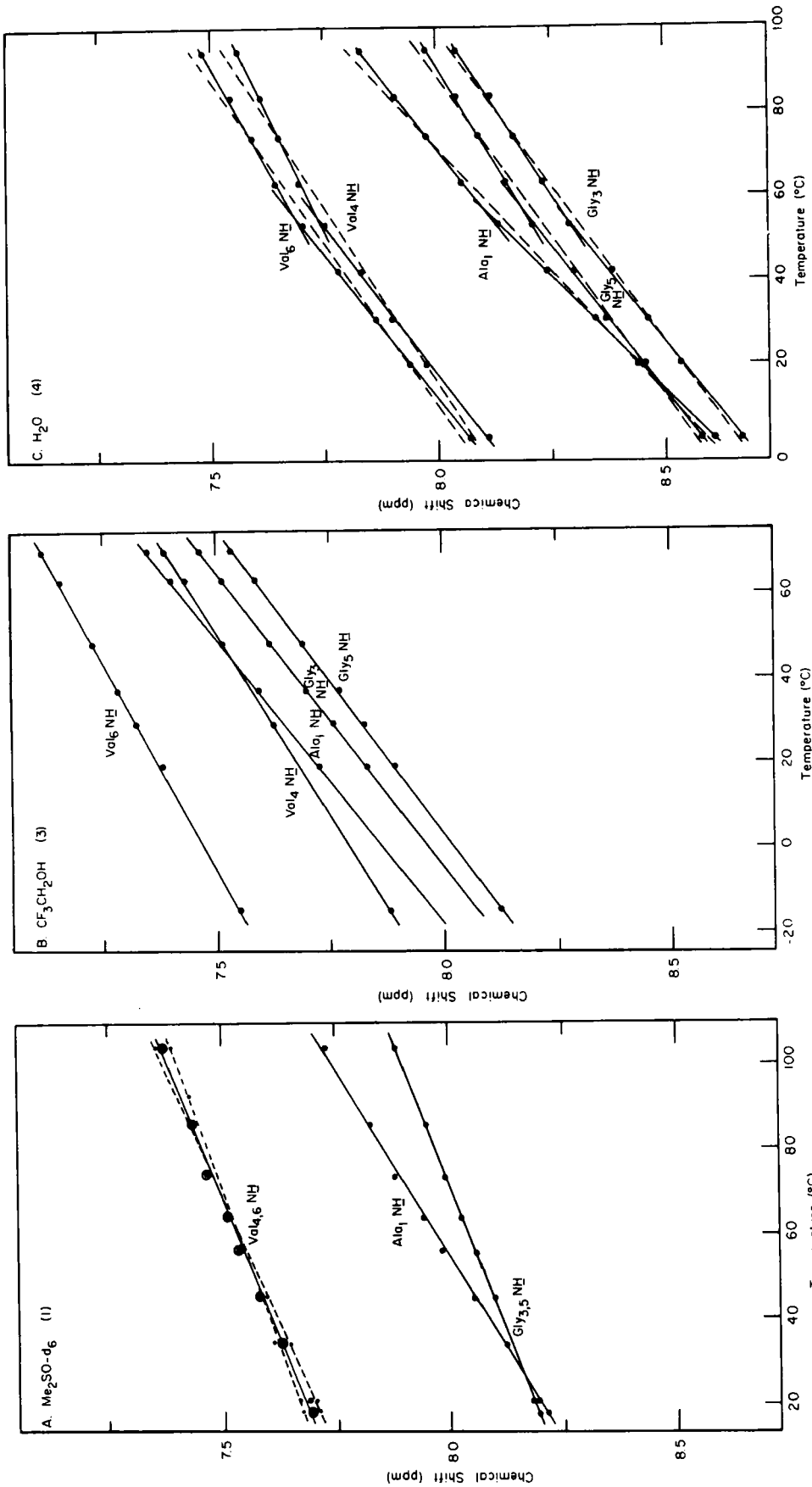

FIGURE 24. Temperature dependence of the proton chemical shift of HCO-Val-(Ala-Pro-Gly-Val-Gly-Val)$_n$-OMe in dimethyl sulfoxide, trifluroethanol, and water.

TABLE 18

Solvent Dependence of HCO-Val-(Ala$_1$-Pro$_2$-Gly$_3$-Val$_4$-Gly$_5$-Val$_6$)-OMe Peptide NH Chemical Shifts at 20°C

PEPTIDE RESIDUE	1 Me_2SO-d_6	2' Me_2SO-d_6: H_2O (1:1)	3 CF_3CH_2OH	4a H_2O	$\Delta\delta/\Delta S_{1,3}$	$\Delta\delta/\Delta S_{1,4a}$	$\Delta\delta/\Delta S_{3,4a}$
Ala_1 NH	8.21	8.33	7.72	8.44	-0.49	0.23	0.72
Gly_3 NH	8.19	8.37	7.84	8.53	-0.35	0.34	0.69
Val_4 NH	7.27	7.79	7.67	7.98	0.40	0.71	0.31
Gly_5 NH	8.19	8.37	7.88	8.46	-0.31	0.27	0.58
Val_6 NH	7.72	7.79	7.37	7.94	-0.35	0.22	0.57

hydrophobic side chains and an association of the hydrophilic groups. This indicates that there is an association of side chains in the conformation at elevated temperatures as was the case with the polypentapeptide (see Figure 17).

The temperature coefficients (slopes) and 0°C intercepts calculated from the best least-squares fit of the data are listed in Table 17. The solvent shifts at 20°C are given in Table 18. Continuing the pattern of the previous peptide, it is the residue$_4$ NH (in this case the Val_4 NH) which is uniformly shown to be solvent shielded. It should be noted that the Val_6 NH of the polyhexapeptide is relatively more shielded in Me_2SO-d_6 and water than it is in the monomer (compare Tables 13 and 17).

The valyl αCH-NH coupling constants are well resolved in the Me_2SO-d_6:H_2O (1:1) solvent system (at 62°C), as well as in water in both the low and high temperature ranges (up to 74°C). In these solvent states both the Val_4 NH and Val_6 NH resonances exhibit $^3J_{\alpha CH\text{-}NH}$ values of 8.5 Hz. The αCH-NH coupling constant for Ala_1 is well resolved in water at 63°C where it is seen to be about 6 Hz. It is necessary that a proposed conformation be consistent with this data which provide information on the αCH-NH dihedral angle.[55]

2. Carbon-13 Magnetic Resonance Studies

The CMR spectrum of HCO-Val-(Ala$_1$-Pro$_2$-Gly$_3$-Val$_4$-Gly$_5$-Val$_6$)$_{18}$-OMe is shown in Figure 25 with all the resonances assigned. The upfield resonances (< 60 ppm) were assigned by comparison with the previous peptides. The carbonyl carbon resonances were assigned in part by carbon-13 enrichment. The Gly_3 ^{13}C-O was enriched to 2%, the Gly_5 ^{13}C-O was enriched to 3%, and the Ala_1 ^{13}C-O was enriched to 4%. This enrichment provides unambiguous assignment of these three carbonyl carbons. The Pro_2 C-O is at its characteristically low field position and is readily assigned. The Val_4 C-O corresponds exactly to the Val_4 C-O of the hexapeptide (compare Tables 15 and 19) and also corresponds to the position of the Val_4 C-O of the polypentapeptide (compare Tables 12 and 19). The remaining resonance in Me_2SO-d_6 is at 120.17 ppm and by elimination is the Val_6 C-O.

The chemical shifts of the carbonyl carbon resonances in Me_2SO-d_6, CF_3CD_2OD, and D_2O (at 23°C and 70°C) are listed in Table 19A, while the solvent shifts are listed in Table 19B. The most solvent shielded carbonyl carbon is the Ala_1 C-O followed by the Val_6 C-O and then by the Gly_5 C-O. The most significant solvent shifts between the low and high temperature ranges in D_2O are an increase in shielding of the Val_6 C-O and Val_4 C-O resonances, making the Val_6 C-O resonance essentially as shielded as the Ala_1 C-O.

3. Comparison of Shielding of Peptide NH and Peptide C-O Resonances and Proposed β-Spiral Conformation

The calculated mole fractions of shielding of the peptide NH and peptide C-O moieties are given in Table 20. In Part A, the Val_4 NH stands out with a calculated value for a totally solvent shielded peptide NH in both Me_2SO-d_6 and H_2O at elevated temperatures. In Part B, the Ala_1 C-O has a calculated value which indicates almost total shielding. Therefore, again we propose the $Ala_{1,i}$ C-O···HN $Val_{4,i}$ β-turn conformational feature shown in Figure 26. The next most shielded peptide NH is that of the Val_6 residue and it is

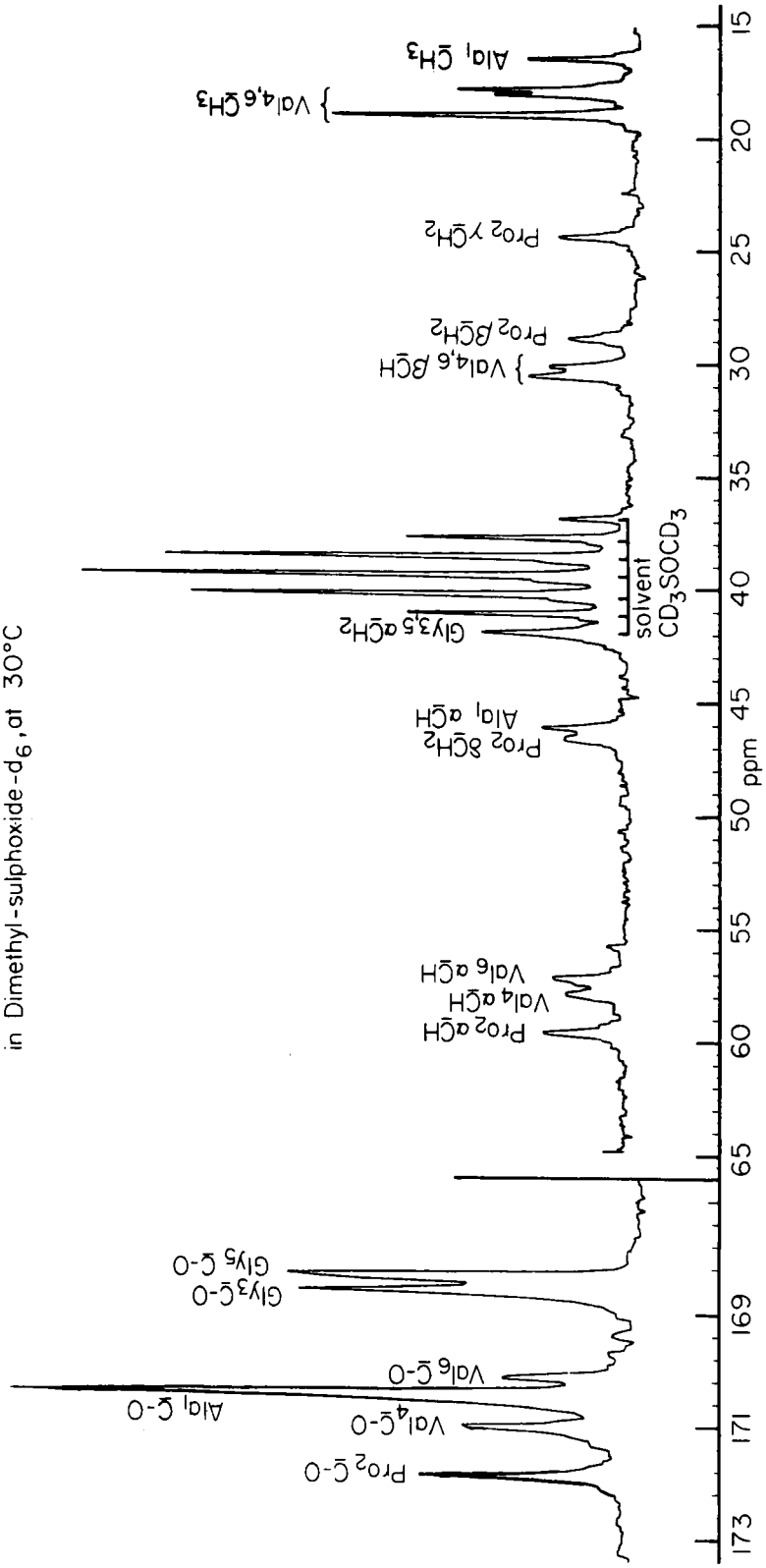

FIGURE 25. Carbon-13 magnetic resonance spectrum at 25 MHz of the elastin polyhexapeptide, HCO-Val-(Ala$_1$-Pro$_2$-Gly$_3$-Val$_4$-Gly$_5$-Val$_6$)$_{1\,8}$-OMe, in Me_2SO-d_6 at 30°C. Chemical shifts are given with respect to an internal reference of TMS. There are no resonances observed between 65 ppm and 168 ppm because the terminal formyl HCO is too weak to detect.(From Urry, D. W., Ohnishi, T., Long, M. M., and Mitchell, L. W., *Int. J. Pept. Protein Res.*, 7, 367, 1975. With permission.)

TABLE 19

Solvent Dependence of HCO-Val-(Ala_1-Pro_2-Gly_3-Val_4-Gly_5-Val_6)$_{1,8}$-OMe Peptide Carbonyl Carbon Chemical Shifts

A. Chemical shifts

PEPTIDE RESIDUE	1 Me_2SO-d_6	3 CF_3CD_2OD	4a D_2O (23°C)	4b D_2O (75°C)
Ala_1 C-O	170.46	173.71	173.71	173.23
Pro_2 C-O	171.87	176.09	175.95	175.37
Gly_3 C-O	168.62	172.89	172.40	171.97
Val_4 C-O	171.00	175.20	175.03	174.30
Gly_5 C-O	168.33	172.21	172.07	171.63
Val_6 C-O	170.17	173.96	173.71	172.99

B. Solvent shifts

PEPTIDE	1 → 3		1 → 4a		1 → 4b		4a → 4b
RESIDUE	$\Delta\delta/\Delta S_{1,3}$	$\Delta\delta_{m1}$	$\Delta\delta/\Delta S_{1,4a}$	$\Delta\delta_{m1}$	$\Delta\delta/\Delta S_{1,4b}$	$\Delta\delta_{m1}$	
Ala_1 C-O	3.25	0	3.25	0	2.77	0	0
Pro_2 C-O	4.22	0.98	4.08	0.83	3.50	0.73	-0.10
Gly_3 C-O	4.27	1.02	3.78	0.53	3.35	0.56	0.03
Val_4 C-O	4.24	0.99	4.03	0.78	3.30	0.53	-0.25
Gly_5 C-O	3.88	0.63	3.74	0.49	3.30	0.53	0.04
Val_6 C-O	3.79	0.54	3.54	0.29	2.82	0.05	-0.24

TABLE 20

Calculated Mole Fractions of Shielding of HCO-Val-(Ala_1-Pro_2-Gly_3-Val_4-Gly_5-Val_6)$_{1,8}$-OMe Peptide NH and Peptide Carbonyls

A.

PEPTIDE RESIDUE	1 Me_2SO-d_6	3 CF_3CH_2OH	4a H_2O (0-50°C)	4b H_2O (60-100°C)
x_S^T (Ala_1 NH)	0.50	0.10	0	0.43
x_S^T (Gly_3 NH)	0.93	0.28	0.40	0.79
x_S^T (Val_4 NH)	1.0	0.55	0.47	1.0
x_S^T (Gly_5 NH)	0.93	0.28	0.43	0.70
x_S^T (Val_6 NH)	0.93	0.73	0.40	0.85

B.

PEPTIDE RESIDUE	1 → 3	1 → 4a
x_s^{st} (Ala_1 C-O)	0.93	0.81
x_s^{st} (Pro_2 C-O)	0.04	0
x_s^{st} (Gly_3 C-O)	0	0.29
x_s^{st} (Val_4 C-O)	0.03	0.05
x_s^{st} (Gly_5 C-O)	0.35	0.33
x_s^{st} (Val_6 C-O)	0.44	0.53

TABLE 17

Temperature Dependence of HCO-Val-(Ala$_1$-Pro$_2$-Gly$_3$-Val$_4$-Gly$_5$-Val$_6$)$_{1\,8}$-OMe Peptide NH Chemical Shifts

PEPTIDE	Me_2SO-d_6		$Me_2SO-d_6:H_2O(1:1)$		CF_3CH_2OH		$H_2O(0-50^oC)$		$H_2O(50-100^oC)$	
RESIDUE	$d\delta/dT_1$	0^o/Intercept	$d\delta/dT_{1,4}$	0^o/Intercept	$d\delta/dT_3$	0^o/Intercept	$d\delta/dT_{4a}$	0^o/Intercept	$d\delta/dT_{4b}$	0^o/Intercept
Ala_1 NH	-5.7	8.32	-7.6	8.48	-7.4	7.87	-9.3	8.63	-7.2	8.51
Gly_3 NH	-3.7	8.26	-5.4	8.48	-6.9	7.98	-7.3	8.68	-5.5	8.50
Val_4 NH	-3.4	7.34	-3.8	7.87	-5.8	7.79	-7.0	8.12	-4.5	7.98
Gly_5 NH	-3.7	8.26	-5.4	8.48	-6.9	8.02	-7.2	8.60	-5.9	8.60
Val_6 NH	-3.7	7.79	-5.3	7.90	-5.1	7.47	-7.3	8.09	-5.2	7.97

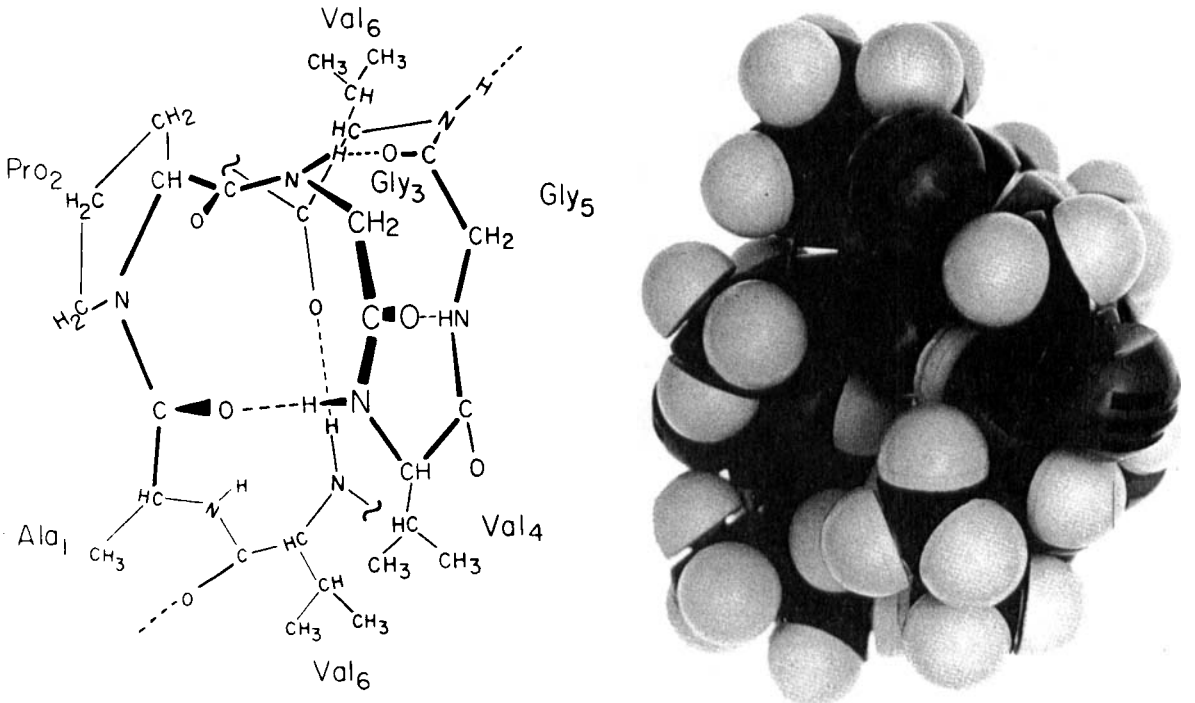

FIGURE 26. Proposed conformation of the repeat hexapeptide in the polyhexapeptide of elastin in its more ordered state. The probability of occurrence of the β-turn is essentially one. In Me_2SO-d_6 and Me_2SO-d_6:H_2O, 1:1 the probabilities of occurrence of the other three hydrogen bonds is greater than 0.7. (From Urry, D. W., Ohnishi, T., Long, M. M., and Mitchell, L. W., *Int. J. Pept. Protein Res.*, 7, 367, 1975. With permission.)

obvious to consider the possibilities of this shielding by the Val_6 C-O which is the next most shielded carbonyl moiety and which exhibits a shielding at elevated temperatures in D_2O which is equivalent to that of the Ala_1 C-O. The question is which Val_6 NH pairs with which Val_6 C-O. If we accept the restriction which was so strictly indicated for the hexapeptide that the Gly_5 C-O be hydrogen bonded to the Gly_3 NH, and which allowed a good description of the polypentapeptide data, then there is a great deal of limitation placed on the Val_6 NH, Val_6 C-O pairing. This extent of shielding is not to be expected from a five-atom hydrogen bonded ring of $Val_{6,i}$ C-O · · · HN $Val_{6,i}$. Given the other two hydrogen bonds of the hexamer and the pentapeptide, a $Val_{6,i}$ C-O · · · HN $Val_{6,i-1}$ would seem to fit the data well. The result is another β-spiral structure shown in Figure 27.

When the structure is shown with a twofold screw symmetry axis as in Figure 27, there is 4.7 Å/hexapeptide repeat along the spiral axis. The plane of the β-turn, Ala_1 C-O · · · HN Val_4, makes an angle of about 40 to 45° with the spiral axis and defines the plane of a hydrophobic ridge which traverses the structure. The perpendicular distances between consecutive ridges on each side is about 6.5 Å. In this structure the valyl αCH-NH dihedral angles are very nearly 180°, whereas the alanyl αCH-NH dihedral angle is about 140°. Both of these values fit well with the PMR coupling constant data of a $^3J_{\alpha CH\text{-}NH}$ for both valyl residues of 8.5 Hz and a $^3J_{\alpha CH\text{-}NH}$ for the alanyl residue of 6 Hz. In addition, a small rotation of the Val_4 C-O brings it into the proximity of the Ala_1 NH which would be consistent with an increased shielding of these moieties on raising the temperature in water.

VI. RELEVANCE OF THE REPEAT PEPTIDE SOLUTION CONFORMATIONS TO FIBROUS ELASTIN

Fibrous elastin occurs in an aqueous milieu at body temperature (37°C); it contains 60% water by volume, and is filamentous exhibiting fibril widths of the order of 30 to 50 Å with a twisted rope appearance.[57] When an aqueous solution of α-elastin or the precursor protein is raised to 37°C, a phase separation occurs. The viscous, more dense phase is called the coacervate. The coacervate of

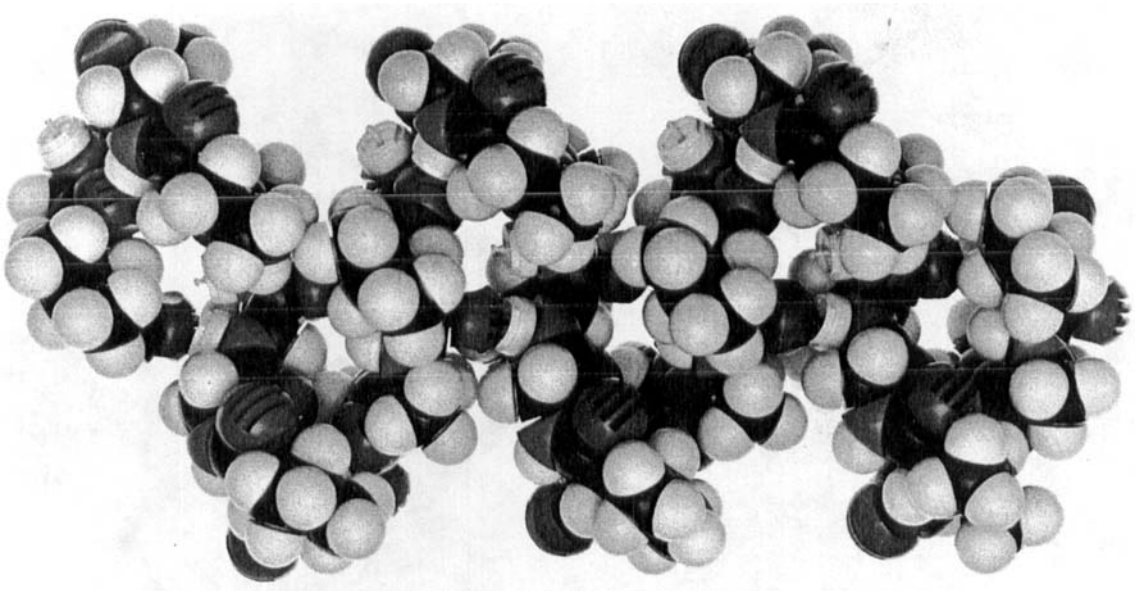

FIGURE 27. Proposed β-spiral conformation for the polyhexapeptide of elastin. The structure has a twofold symmetry axis with a 4.7 A translation along the axis for each repeat. In addition, hydrophobic ridges form at about 40° to the helix axis and occur at 6.5-A intervals. It is possible that the structure would relax to 2.2 residues per turn giving a 4.4 A for the repeat distance. (From Urry, D. W,, Ohnishi, T., Long, M. M., and Mitchell, L. W., *Int. J. Pept. Protein Res.*, 7, 367, 1975. With permission.)

α-elastin is 60% water by volume, is the stable state at body temperature, and is filamentous with repeats similar to those of fibrous elastin.[58,59] Thus, the coacervate is a model for the fibrous state. The filamentous ordering with increasing temperature and circular dichroism studies[60] indicate an increase in order on coacervation, both intermolecularly and intramolecularly. The concentration dependent process may be interpreted as intermolecular hydrophobic association between elements forming the filaments as discussed previously.

Raising the temperature of a several hundred milligrams per milliliter solution of the polytetrapeptide results in no phase separation. The solution remains clear and homogeneous. Raising the temperature of aqueous solutions of the polypentapeptide and the polyhexapeptide results in initial clouding and phase separation. With $\bar{n} \cong 18$, the concentration which remains in the supernatant above the polypentapeptide coacervate is about 20 mg/ml. It is this supernatant for which the data in water at elevated temperatures have been reported. It is important to note that the coacervate is the stable state at 37°C in an aqueous system; it contains about 60% water by volume, and is filamentous.[61] Thus, the coacervate of the polypentapeptide is very similar not only to the coacervate of α-elastin and tropoelastin, but also to fibrous elastin and may reasonably be considered a satisfactory model for fibrous elastin.

The coacervate, though 60% water by volume, is a state with predominant hydrophobic interactions. This makes the data in the organic solvents of heightened interest. In this regard in Table 20A the similarity of shielding of the peptide NHs in $Me_2SO\text{-}d_6$ and water at elevated temperatures is striking, suggesting that similar conformations exist in the two solvent states. It may also be noted that fibrous elastin is a more ideal elastomer in $Me_2SO\text{-}d_6$ than in water.[62] Thus there is good reason to consider both the $Me_2SO\text{-}d_6$ and the water (at elevated temperatures) conformations as being relevant to fibrous elastin.

In a highly detailed analysis of the twisted rope appearance of elastin fibrils, Volpin and Gotte[63] describe the twisted rope appearance as derived from 15-Å filaments twisted around each other. Also in his analysis of the diffusion of solutes through fibrous elastin, Partridge[56] considered a 16-Å filament as consistent with the data. Both the working model of the polypentapeptide in Figure 17 and the working model of the polyhexa-

peptide in Figure 27 could self-associate or even co-associate with one chain twisted around the other with the requisite intermolecular hydrophobic interactions and with a twist period of about 100 Å, which would be consistent with the high resolution electron microscope data.[57] Thus we view the fine structure of the elastic fiber in its more ordered regions as being comprised of hydrophobically associating chains in a β-spiral structure which are twisted around each other with periods of about 100 Å to give a twisted rope appearance. In series with such regions are cross-linking regions which, as proposed by Gray et al.,[33] probably are α-helical segments with two helices being covalently attached by a desmosine or isodesmosine cross-link. This series arrangement of β-spiral and α-helical segments has been proposed previously.[36] What we are now able to add is greater detail in the description of the β-spiral segments.

ACKNOWLEDGMENT

The authors gratefully acknowledge L. W. Mitchell for superb technical assistance on the CMR.

REFERENCES

1. **Urry, D. W.,** On the molecular basis for vascular calcification, *Perspect. Biol. Med.,* 18(1), 68, 1974.
2. **Robert, L., Robert, B., and Robert, A. M.,** Molecular biology of elastin as related to aging and atherosclerosis, *Exp. Gerontol.,* 5, 339, 1970.
3. **Blumenthal, H. T., Lansing, A. I., and Wheeler, P. A.,** Calcification of the media of the human aorta and its relation to intimal arteriosclerosis, ageing and disease, *Am. J. Pathol.,* 20, 665, 1944.
4. **Lansing, A. I., Blumenthal, H. T., and Gray, S. H.,** Ageing and calcification of the human coronary artery, *J. Gerontol.,* 3, 87, 1948.
5. **Lansing, A. I., Alex, M., and Rosenthal, T. B.,** Calcium and elastin in human arteriosclerosis, *J. Gerontol.,* 5, 112, 1949–50.
6. **Blumenthal, H. T., Lansing, A. I., and Gray, S. H.,** The interrelation of elastic tissue and calcium in the genesis of atherosclerosis, *Am. J. Pathol.,* 26, 989, 1950.
7. **Lansing, A. I.,** Elastic tissue in atherosclerosis, in *Connective Tissue, Thrombosis and Atherosclerosis,* Page, I. H., Ed., Academic Press, New York, 1959, 167.
8. **Yu, S. Y. and Blumenthal, H. T.,** The calcification of elastic fibers. I. Biochemical studies, *J. Gerontol.,* 18, 119, 1963.
9. **Yu, S. Y. and Blumenthal, H. T.,** The calcification of elastic fibers. II. Ultramicroscope characteristics, *J. Gerontol.,* 18, 127, 1963.
10. **McCarthy, J. H. and Palmer, F. J.,** Incidence and significance of coronary artery calcification, *Br. Heart J.,* 36, 499, 1974.
11. **Meyer, W. W. and Lind, J.,** Iliac arteries in children with a single umbilical artery, structure, calcification and early atherosclerotic lesions, *Arch. Dis. Child.,* 49, 671, 1974.
12. **Eisenstein, R., Ayer, J. P., Papajiannis, S., Hass, G. M., and Ellis, H.,** Mineral binding by human arterial tissue, *Lab. Invest.,* 13, 1198, 1964.
13. **Martin, G. R., Schiffmann, E., Bladen, H. A., and Nylen, M.,** Chemical and morphological studies on the in vitro calcification of aorta, *J. Cell. Biol.,* 16, 243, 1963.
14. **Klotz, O. and Manning, M. F.,** Fatty streaks in the intima of arteries, *J. Pathol. Bacteriol.,* 16, 211, 1911.
15. **Klotz, O.,** Fatty degeneration of the intima of arteries, *J. Med. Res.,* 32, 27, 1915.
16. **Parker, F.,** An electron microscope study of experimental atherosclerosis, *Am. J. Pathol.,* 36, 19, 1960.
17. **Adams, C. W. M. and Tuqans, N. A.,** Elastic degeneration as source of lipids in the early lesion of atherosclerosis, *J. Pathol. Biol.,* 82, 131, 1961.
18. **Friedman, M.,** Pathogenesis of the spontaneous atherosclerotic plaque, *Arch. Pathol.,* 76, 318, 1963.
19. **Kramsch, D. M., Franzblau, C., and Hollander, W.,** The protein and lipid composition of arterial elastin and its relationship to lipid accumulation in the atherosclerotic plaque, *J. Clin. Invest.,* 50, 1666, 1971.
20. **Kramsch, D. M. and Hollander, W.,** The interaction of serum and arterial lipoproteins with elastin of the arterial intima and its role in the lipid accumulation in atherosclerotic plaques, *J. Clin. Invest.,* 52, 236, 1973.
21. **Jacotot, B., Beaumont, J. L., Munnier, G., Szigeti, M., Robert, B., and Robert, L.,** Role of elastic tissue in cholesterol deposition in the arterial wall, *Nutr. Metab.,* 15, 46, 1973.

22. **Spaet, T. H. and Erichson, R. B.,** The vascular wall in the pathogenesis of thrombosis, *Thromb. Diath. Haemorrh. Suppl.*, 21, 67, 1966.
23. **Kabemba, J. M., Mayer, J. E., and Hammond, G. L.,** Experimental arterial thrombosis formation in vivo by proteolytic enzyme perfusion and the role of elastin layer, *Surgery*, 73(3), 438, 1973.
24. **Urry, D. W.,** Molecular aspects of the elastic fiber as a site of vascular pathology, *Ala. J. Med. Sci.*, 12(4), 361, 1975.
25. **Gotte, L., Mammi, M., and Pezzin, G.,** Scanning electron microscope observations on elastin, *Connect. Tissue Res.*, 1, 61, 1972.
26. **Ross, R.,** The elastic fiber, *J. Histochem. Cytochem.*, 21, 199, 1973.
27. **Partridge, S. M.,** Elastin, biosynthesis and structure, *Gerontologia*, 15, 85, 1969.
28. **Franzblau, C. and Lent, R. W.,** Studies on the chemistry of elastin. *Brookhaven Symp. Biol. – Structure, Function Evolution of Proteins*, 21, 358, 1969.
29. **Sandberg, L. B., Weissman, N., and Gray, W. R.,** Structural features of tropoelastin related to the sites of cross-links in aortic elastin, *Biochemistry*, 10, 52, 1971.
30. **Foster, J. A., Rubin, L., Kagan, H. M., Franzblau, C., Bruenger, E., and Sandberg, L. B.,** Isolation and characterization of cross-linked peptides from elastin, *J. Biol. Chem.*, 249(19), 6191, 1974.
31. **Sandberg, L. B., Weissman, N., and Smith, D. W.,** The purification and partial characterization of a soluble elastin-like protein from copper deficient porcine aorta, *Biochemistry*, 8, 2940, 1969.
32. **Smith, D. W., Weissman, N., and Carnes, W. H.,** Cardiovascular studies on copper deficient swine. XII. Partial purification of a soluble protein resembling elastin, *Biochem. Biophys. Res. Commun.*, 31, 309, 1968.
33. **Gray, W. R., Sandberg, L. B., and Foster, J. A.,** Molecular model for elastin structure and function, *Nature*, 246, 461, 1973.
34. **Foster, J. A., Bruenger, E., Gray, W. R., and Sandberg, L. B.,** Isolation and amino acid sequences of tropoelastin peptides, *J. Biol. Chem.*, 248, 2876, 1973.
35. **Urry, D. W., Cunningham, W. D., and Ohnishi, T.,** A neutral polypeptide-calcium ion complex, *Biochim. Biophys. Acta Rep.*, 292, 853, 1973.
36. **Urry, D. W.,** Studies on the conformation and interactions of elastin, in *Arterial Mesenchyme and Arteriosclerosis*, by Wagner, W. D. and Clarkson, T. B., Eds., *Adv. Exp. Med. Biol.*, 43, 211, 1974.
37. **Urry, D. W., Cunningham, W. D., and Ohnishi, T.,** Studies on the conformation and interactions of elastin. Proton magnetic resonance of repeating pentapeptide, *Biochemistry*, 13, 609, 1974.
38. **Urry, D. W. and Ohnishi, T.,** Studies on the conformations and interactions of elastin. Proton magnetic resonance of the repeating tetramer, *Biopolymers*, 13, 1223, 1974.
39. **Urry, D. W. and Ohnishi, T.,** Recurrence of β turns in repeat peptides of elastin: The hexapeptide Ala-Pro-Gly-Val-Gly-Val sequences and derivatives, in *Peptides, Polypeptides and Proteins*, Blout, E. R., Bovey, F. A., Goodman, M., and Lotan, N., Eds., John Wiley & Sons, New York, 1974, 230.
40. **Long, M. M., Urry, D. W., and Ohnishi, T.,** Circular dichroism of repeat pentapeptide of elastin, *Int. Res. Commun. Syst.*, 2, 1352, 1974.
41. **Urry, D. W., Mitchell, L. W., and Ohnishi, T.,** Carbon-13 magnetic resonance evaluation of polypeptide secondary structure and correlation with proton magnetic resonance studies, *Proc. Natl. Acad. Sci. USA*, 71(8), 3265, 1974.
42. **Urry, D. W., Mitchell, L. W., and Ohnishi, T.,** Solvent dependence of peptide carbonyl carbon chemical shifts and polypeptide secondary structure: The repeat tetrapeptide of elastin, *Biochem. Biophys. Res. Commun.*, 59, 62, 1974.
43. **Urry, D. W., Mitchell, L. W., and Ohnishi, T.,** Carbon-13 magnetic resonance assignments of the repeat peptides of elastin and solvent delineation of carbonyls, *Biochemistry*, 13, 4083, 1974.
44. **Urry, D. W., Long, M. M., Cox, B. A., Ohnishi, T., Mitchell, L. W., and Jacobs, M.,** The synthetic polypentapeptide of elastin coacervates and forms filamentous aggregates, *Biochim. Biophys. Acta*, 371(2), 597, 1974.
45. **Urry, D. W., Long, M. M., Ohnishi, T., and Jacobs, M.,** Circular dichroism and absorption of the polytetrapeptide of elastin: A polymer model for the β-turn, *Biochem. Biophys. Res. Commun.*, 61(4), 1427, 1974.
46. **Urry, D. W., Mitchell, L. W., and Ohnishi, T.,** Studies on the conformation and interactions of elastin: Secondary structure of synthetic repeat hexapeptides, *Biochim. Biophys. Acta*, 393, 296, 1975.
47. **Urry, D. W., Ohnishi, T., Long, M. M., and Mitchell, L. W.,** Studies on the conformation and interactions of elastin: Nuclear magnetic resonance of the polyhexapeptide, *Int. J. Pept. Protein Res.*, 7, 367, 1975.
48. **Urry, D. W., Mitchell, L. W., Ohnishi, T., and Long, M. M.,** Proton and carbon magnetic resonance studies of the synthetic polypentapeptide of elastin, *J. Mol. Biol.*, 96, 101, 1975.
49. **Urry, D. W.,** Nuclear magnetic resonance and the conformation of membrane active peptides, in *Membrane Bound Enzymes*, Martonosi, A., Ed., Plenum Press, New York, 1975.
50. **Urry, D. W., Long, M. M., Mitchell, L. W., and Okamoto, K.,** Utilization of proton and carbon-13 magnetic resonance in the evaluation of polypeptide secondary structure in solution, in *Peptides: Chemistry, Structure and Biology*, Walter, R., and Meienhofer, J., Eds., Ann Arbor Science Publishers, Ann Arbor, Michigan, 1975.
51. **Urry, D. W. and Ohnishi, M.,** Nuclear magnetic resonance and the conformation of cyclic polypeptide antibiotics, in *Spectroscopic Approaches to Biomolecular Conformation*, Urry, D. W., Ed., American Medical Association Press, Chicago, Ill., 1970, 263.

52. **Pease, L. G., Deber, C. M., and Blout, E. R.,** Cyclic Peptides. V. ^{1}H and ^{13}C Nuclear magnetic resonance determination of the preferred β conformation for proline-containing cyclic hexapeptides, *J. Am. Chem. Soc.*, 95, 258, 1973.
53. **Partridge, S. M., Davis, H. F., and Adair, G. S.,** The chemistry of connective tissues. 2. Soluble proteins derived from partial hydrolysis of elastin, *Biochem. J.*, 61, 11, 1955.
54. **Partridge, S. M. and Davis, H. F.,** The chemistry of connective tissue. 3. Composition of the soluble proteins derived from elastin, *Biochem. J.*, 61, 21, 1955.
55. **Ramachandran, G. N., Chandrasekaran, R., and Kopple, K. D.,** Variation of the NH-CαH coupling constant with dihedral angle in the NMR spectra of peptides, *Biopolymers*, 10, 2113, 1971.
56. **Partridge, S. M.,** Diffusion of solutes in elastin fibers, *Biochim. Biophys. Acta*, 140, 132, 1967.
57. **Gotte, L., Giro, M. G., Volpin, D., and Horne, R. W.,** The ultrastructural organization of elastin, *J. Ultrastruct. Res.*, 46, 23, 1974.
58. **Cox, B. A., Starcher, B. C., and Urry, D. W.,** Coacervation of tropoelastin results in fiber formation, *J. Biol. Chem.*, 249, 997, 1974.
59. **Cox, B. A., Starcher, B. C., and Urry, D. W.,** Coacervation of α-elastin results in fiber formation, *Biochim. Biophys. Acta*, 317, 209, 1973.
60. **Starcher, B. C., Saccomani, G., and Urry, D. W.,** Coacervation and ion binding studies on aortic elastin, *Biochim. Biophys. Acta*, 310, 481, 1973.
61. **Urry, D. W., Long, M. M., Cox, B. A., Ohnishi, T., Mitchell, L. W., and Jacobs, M.,** The synthetic polypentapeptide of elastin coacervates and forms filamentous aggregates, *Biochim. Biophys. Acta*, 371, 597, 1974.
62. **Mistrali, F., Volpin, D., Garibaldi, G. B., and Ciferri, A.,** Thermodynamics of elasticity in open systems. Elastin, *J. Phys. Chem.*, 75, 142, 1971.
63. **Gotte, L., Volpin, D., Horne, R. W., and Mammi, M.,** Electron microscopy and optical diffraction of elastin, *Micron*, in press, 1976.
64. **Urry, D. W.,** Studies on the conformations and interactions of elastin, in *Arterial Mesenchyme and Arteriosclerosis*, Wagner, W. D. and Clarkson, T. B., Eds., *Adv. Exp. Med. Biol.*, 43, 211, 1974.